

This is the accepted manuscript made available via CHORUS. The article has been published as:

# Classically conformal $U(1)^{\prime}$ extended standard model, electroweak vacuum stability, and LHC Run-2 bounds

Arindam Das, Satsuki Oda, Nobuchika Okada, and Dai-suke Takahashi

Phys. Rev. D **93**, 115038 — Published 29 June 2016

DOI: [10.1103/PhysRevD.93.115038](https://doi.org/10.1103/PhysRevD.93.115038)

# Classically conformal $U(1)'$ extended standard model, electroweak vacuum stability, and LHC Run-2 bounds

Arindam Das <sup>a 1</sup>, Satsuki Oda <sup>b,c 2</sup>, Nobuchika Okada <sup>a 3</sup>,  
and Dai-suke Takahashi <sup>b,c 4</sup>

<sup>a</sup>*Department of Physics and Astronomy, University of Alabama,  
Tuscaloosa, Alabama 35487, USA*

<sup>b</sup>*Okinawa Institute of Science and Technology Graduate School (OIST),  
Onna, Okinawa 904-0495, Japan*

<sup>c</sup>*Research Institute, Meio University,  
Nago, Okinawa 905-8585, Japan*

## Abstract

We consider the minimal  $U(1)'$  extension of the Standard Model (SM) with the classically conformal invariance, where an anomaly free  $U(1)'$  gauge symmetry is introduced along with three generations of right-handed neutrinos and a  $U(1)'$  Higgs field. Since the classically conformal symmetry forbids all dimensional parameters in the model, the  $U(1)'$  gauge symmetry is broken through the Coleman-Weinberg mechanism, generating the mass terms of the  $U(1)'$  gauge boson ( $Z'$  boson) and the right-handed neutrinos. Through a mixing quartic coupling between the  $U(1)'$  Higgs field and the SM Higgs doublet field, the radiative  $U(1)'$  gauge symmetry breaking also triggers the breaking of the electroweak symmetry. In this model context, we first investigate the electroweak vacuum instability problem in the SM. Employing the renormalization group equations at the two-loop level and the central values for the world average masses of the top quark ( $m_t = 173.34$  GeV) and the Higgs boson ( $m_h = 125.09$  GeV), we perform parameter scans to identify the parameter region for resolving the electroweak vacuum instability problem. Next we interpret the recent ATLAS and CMS search limits at the LHC Run-2 for the sequential  $Z'$  boson to constrain the parameter region in our model. Combining the constraints from the electroweak vacuum stability and the LHC Run-2 results, we find a bound on the  $Z'$  boson mass as  $m_{Z'} \gtrsim 3.5$  TeV. We also calculate self-energy corrections to the SM Higgs doublet field through the heavy states, the right-handed neutrinos and the  $Z'$  boson, and find the naturalness bound as  $m_{Z'} \lesssim 7$  TeV, in order to reproduce the right electroweak scale for the fine-tuning level better than 10%. The resultant mass range of  $3.5 \text{ TeV} \lesssim m_{Z'} \lesssim 7 \text{ TeV}$  will be explored at the LHC Run-2 in the near future.

---

<sup>1</sup>adas8@ua.edu

<sup>2</sup>satsuki.oda@oist.jp

<sup>3</sup>okadan@ua.edu

<sup>4</sup>daisuke.takahashi@oist.jp

# 1 Introduction

One of the most serious problems in the standard model (SM) is the so-called gauge hierarchy problem, which has been motivating us to seek new physics beyond the SM for decades. The problem originates from the fact that quantum corrections to the self-energy of the SM Higgs doublet field quadratically diverge, and this divergence, once cut off by a physical new physics scale being much higher than the electroweak scale, must be canceled by a fine-tuning of the Higgs mass parameter at the tree level. Because of the chiral nature of the SM, the SM Lagrangian possesses the conformal (scale) invariance at the classical level, except for the Higgs mass term. It has been argued in [1] that once the classically conformal invariance and its minimal violation by quantum anomalies are imposed on the SM, it could be free from the quadratic divergences and hence, the classically conformal invariance might provide us with a solution to the gauge hierarchy problem. This picture nicely fits a setup first investigated by Coleman and Weinberg [2], namely, a  $U(1)$  gauge theory with a massless Higgs field. In this setup, it has been shown that the  $U(1)$  gauge symmetry is radiatively broken in the Coleman-Weinberg effective potential (Coleman-Weinberg mechanism).

Although it is tempting to apply this Coleman-Weinberg mechanism to the SM Higgs sector, this cannot work with the observed values of top quark and weak boson masses, since the Coleman-Weinberg potential for the SM Higgs field is found to be unbounded from below [3]. Therefore, in order to pursue this scheme, it is necessary to extend the SM. There have been a lot of new physics model proposals (see, for example, [4, 5, 6]). In this paper, we consider the classically conformal  $U(1)'$  extension of the SM proposed in [7], where in addition to the SM particle contents, three generations of right-handed neutrinos and a  $U(1)'$  Higgs field are introduced. By assigning generation-independent  $U(1)'$  charges for fermions and requiring to reproduce the Yukawa structure in the SM and to make the model free from all gauge and gravitational anomalies, it turns out that the  $U(1)'$  gauge symmetry is identified as a linear combination of the SM  $U(1)_Y$  and the  $U(1)_{B-L}$  gauge groups [8]. Hence, our model is a generalization on the classically conformal  $U(1)_{B-L}$  extension of the SM proposed in [6]. The  $U(1)'$  gauge symmetry is radiatively broken by the Coleman-Weinberg mechanism, and the  $U(1)'$  gauge field ( $Z'$  boson) and the right-handed (Majorana) neutrinos acquire their masses. A mixing quartic coupling between the  $U(1)'$  Higgs and the SM Higgs doublet fields generates a negative mass squared for the SM Higgs doublet field, and the electroweak symmetry breaking is driven. Therefore, the radiative  $U(1)'$  gauge symmetry is the sole origin of the mass scale in this model. With the Majorana heavy neutrinos, the seesaw mechanism [9] is automatically implemented and tiny active neutrino masses and their flavor mixing are generated after the electroweak symmetry breaking.

The SM Higgs boson has been discovered at the LHC, and this marks the beginning of the experimental confirmation of the SM Higgs sector. The observed Higgs boson mass of  $m_h = 125.09 \pm 0.21(\text{stat.}) \pm 0.11(\text{syst.})$  GeV from a combined analysis by the ATLAS and the CMS [10] indicates that the electroweak vacuum is unstable [11], since the SM Higgs quartic coupling becomes negative far below the Planck mass, for the top quark pole mass  $m_t = 173.34 \pm 0.76$  from the combined measurements by the Tevatron and the LHC experiments [12]. Practically, this instability may not be a problem in the SM, since the lifetime of our electroweak vacuum is estimated to be much longer than the age of the universe [13]. However,

in the presence of the  $U(1)'$  Higgs field, our Higgs potential is a function of two Higgs fields, and there might be a path to avoid hills and make the lifetime of our electroweak vacuum very short. Because of a lack of field theoretical technology for analyzing the effective scalar potential with multi-scalars in a wide range of field values, it would be the best way to solve the electroweak vacuum instability problem in the context of our model.

In this paper, we investigate the electroweak vacuum stability in the classically conformal  $U(1)'$  extended SM. In the same model context, the electroweak vacuum stability problem and the current experimental bounds on the model have been investigated in [7]. The purpose of the present paper is to improve the analysis in [7] for the electroweak vacuum stability by the renormalization group equations (RGEs) at the two-loop level, and present a complete result for the parameter scan. We also update the constraints on the model parameters by taking into account the recent LHC Run-2 results on search for  $Z'$  boson resonances [17, 18]. We will find that the LHC Run-2 results dramatically improve those obtained from the Run 1 results. In addition, we calculate the SM Higgs self-energy corrections from the effective potential involving the heavy states, the right-handed neutrinos and the  $Z'$  boson, after the  $U(1)'$  symmetry breaking, and derive the naturalness bounds to reproduce the right electroweak scale for the fine-tuning level better than 10%.

This paper is organized as follows. Our  $U(1)'$  model is defined in the next section. In Sec. 3, we discuss the radiative  $U(1)'$  symmetry breaking through the Coleman-Weinberg mechanism. The electroweak symmetry breaking triggered by the radiative  $U(1)'$  gauge symmetry breaking is discussed in Sec. 4. In Sec. 5, we analyze the renormalization group (RG) evolutions of the couplings at the two-loop level, and find a region in 3 dimensional parameter space which can resolve the electroweak vacuum instability and keep all parameters in the perturbative regime up to the Planck mass. In Sec. 6, we analyze the current collider bounds of the model parameters, in particular, the recent ATLAS and CMS results of the search for the  $Z'$  boson resonance at the LHC Run-2 are interpreted to the  $Z'$  boson case of our model. In Sec. 7, we evaluate self-energy corrections to the SM Higgs doublet from the effective potential, and derive the naturalness bounds to reproduce the electroweak scale for the fine-tuning level better than 10%. We summarize our results in Sec. 8. Formulas we used in our analysis are listed in Appendices.

Although Sec. 2 - Sec. 4 substantially overlap with our previous work [7], we have repeated the similar discussions for readers convenience. If a reader is familiar with the basic properties of the classically conformal  $U(1)'$  model discussed in Sec. 2 - Sec. 4, he/she can skip over the sections.

## 2 Classically conformal $U(1)'$ extended SM

The model we will investigate is the anomaly-free  $U(1)'$  extension of the SM with the classically conformal invariance, which is based on the gauge group  $SU(3)_C \times SU(2)_L \times U(1)_Y \times U(1)'$ . The particle contents of the model are listed in Table 1. In addition to the SM particle content, three generations of right-hand neutrinos  $\nu_R^i$  and a  $U(1)'$  Higgs field  $\Phi$  are introduced. The

	SU(3) <sub>c</sub>	SU(2) <sub>L</sub>	U(1) <sub>Y</sub>	U(1)'	
$q_L^i$	<b>3</b>	<b>2</b>	+1/6	$x_q =$	$\frac{1}{3}x_H + \frac{1}{6}x_\Phi$
$u_R^i$	<b>3</b>	<b>1</b>	+2/3	$x_u =$	$\frac{4}{3}x_H + \frac{1}{6}x_\Phi$
$d_R^i$	<b>3</b>	<b>1</b>	-1/3	$x_d =$	$-\frac{2}{3}x_H + \frac{1}{6}x_\Phi$
$\ell_L^i$	<b>1</b>	<b>2</b>	-1/2	$x_\ell =$	$-x_H - \frac{1}{2}x_\Phi$
$\nu_R^i$	<b>1</b>	<b>1</b>	0	$x_\nu =$	$-\frac{1}{2}x_\Phi$
$e_R^i$	<b>1</b>	<b>1</b>	-1	$x_e =$	$-2x_H - \frac{1}{2}x_\Phi$
$H$	<b>1</b>	<b>2</b>	+1/2	$x_H =$	$x_H$
$\Phi$	<b>1</b>	<b>1</b>	0	$x_\Phi =$	$x_\Phi$

Table 1: Particle contents. In addition to the SM particle contents, the right-handed neutrino  $\nu_R^i$  ( $i = 1, 2, 3$  denotes the generation index) and a complex scalar  $\Phi$  are introduced.

covariant derivative relevant to  $U(1)_Y \times U(1)'$  are defined as

$$D_\mu \equiv \partial_\mu - i \begin{pmatrix} Y_1 & Y_X \end{pmatrix} \begin{pmatrix} g_1 & g_{1X} \\ g_{X1} & g_X \end{pmatrix} \begin{pmatrix} B_\mu \\ B'_\mu \end{pmatrix}, \quad (2.1)$$

where  $Y_1$  ( $Y_X$ ) are  $U(1)_Y$  ( $U(1)'$ ) charge of a particle, and the gauge coupling  $g_{X1}$  and  $g_{1X}$  are introduced associated with a kinetic mixing between the two  $U(1)$  gauge bosons.

For generation-independent charge assignments, the  $U(1)'$  charges of the fermions are defined to satisfy the gauge and gravitational anomaly-free conditions:

$$\begin{aligned}
U(1)' \times [SU(3)_C]^2 : & \quad 2x_q - x_u - x_d = 0, \\
U(1)' \times [SU(2)_L]^2 : & \quad 3x_q + x_\ell = 0, \\
U(1)' \times [U(1)_Y]^2 : & \quad x_q - 8x_u - 2x_d + 3x_\ell - 6x_e = 0, \\
[U(1)']^2 \times U(1)_Y : & \quad x_q^2 - 2x_u^2 + x_d^2 - x_\ell^2 + x_e^2 = 0, \\
[U(1)']^3 : & \quad 6x_q^3 - 3x_u^3 - 3x_d^3 + 2x_\ell^3 - x_\nu^3 - x_e^3 = 0, \\
U(1)' \times [\text{grav.}]^2 : & \quad 6x_q - 3x_u - 3x_d + 2x_\ell - x_\nu - x_e = 0.
\end{aligned} \quad (2.2)$$

In order to reproduce observed fermion masses and flavor mixings, we introduce the following Yukawa interactions:

$$\mathcal{L}_{\text{Yukawa}} = -Y_u^{ij} \bar{q}_L^i \tilde{H} u_R^j - Y_d^{ij} \bar{q}_L^i H d_R^j - Y_\nu^{ij} \bar{\ell}_L^i \tilde{H} \nu_R^j - Y_e^{ij} \bar{\ell}_L^i H e_R^j - Y_M^i \Phi \bar{\nu}_R^{ic} \nu_R^i + \text{h.c.}, \quad (2.3)$$

where  $\tilde{H} \equiv i\tau^2 H^*$ , and the third and fifth terms in the right-handed side are for the seesaw mechanism to generate neutrino masses. These Yukawa interaction terms impose

$$\begin{aligned}
x_H &= -x_q + x_u = x_q - x_d = -x_\ell + x_\nu = x_\ell - x_e, \\
x_\Phi &= -2x_\nu.
\end{aligned} \quad (2.4)$$

Solutions to these conditions are listed in Table 1, which are controlled by only two parameters,  $x_H$  and  $x_\Phi$ . The two parameters reflect the fact that the  $U(1)'$  gauge group can be defined as

a linear combination of the SM  $U(1)_Y$  and the  $U(1)_{B-L}$  gauge groups. Since the  $U(1)'$  gauge coupling  $g_X$  is a free parameter of the model and it always appears as a product  $x_\Phi g_X$  or  $x_H g_X$ , we fix  $x_\Phi = 2$  without loss of generality throughout this paper. This convention excludes the case that  $U(1)'$  gauge group is identical with the SM  $U(1)_Y$ . The choice of  $(x_H, x_\Phi) = (0, 2)$  corresponds to the  $U(1)_{B-L}$  model. Another example is  $(x_H, x_\Phi) = (-1, 2)$ , which corresponds to the SM with the so-called  $U(1)_R$  symmetry. When we choose  $(x_H, x_\Phi) = (-16/41, 2)$ , the beta function of  $g_{X1}$  ( $g_{1X}$ ) at the 1-loop level has only terms proportional to  $g_{X1}$  ( $g_{1X}$ ) (see Appendix A). This is the orthogonal condition between the  $U(1)_Y$  and  $U(1)'$  at the 1-loop level, under which  $g_{X1}$  and  $g_{1X}$  do not evolve once we have set  $g_{X1} = g_{1X} = 0$  at an energy scale. Although it is slightly modified ( $x_H$  becomes slightly larger than  $-16/41$ ), we find that the choice of  $(x_H, x_\Phi) = (-16/41, 2)$  is a good approximation even at the 2-loop level.

Imposing the classically conformal invariance, the scalar potential is given by

$$V = \lambda_H (H^\dagger H)^2 + \lambda_\Phi (\Phi^\dagger \Phi)^2 + \lambda_{\text{mix}} (H^\dagger H) (\Phi^\dagger \Phi), \quad (2.5)$$

where the mass terms are forbidden by the conformal invariance. If  $\lambda_{\text{mix}}$  is negligibly small, we can analyze the Higgs potential separately for  $\Phi$  and  $H$  as a good approximation. This will be justified in the following sections. When the Majorana Yukawa couplings  $Y_M^i$  are negligible compared to the  $U(1)'$  gauge coupling, the  $\Phi$  sector is identical with the original Coleman-Weinberg model [2], so that the radiative  $U(1)'$  symmetry breaking will be achieved. Once  $\Phi$  develops a vacuum expectation value (VEV) through the Coleman-Weinberg mechanism, the tree-level mass term for the SM Higgs is effectively generated through  $\lambda_{\text{mix}}$  in Eq. (2.5). Taking  $\lambda_{\text{mix}}$  negative, the induced mass squared for the Higgs doublet is negative and, as a result, the electroweak symmetry breaking is driven in the same way as in the SM.

### 3 Radiative $U(1)'$ gauge symmetry breaking

Assuming  $\lambda_{\text{mix}}$  is negligibly small, we first analyze the  $U(1)'$  Higgs sector. Without mass terms, the Coleman-Weinberg potential [2] at the 1-loop level is found to be

$$V(\phi) = \frac{\lambda_\Phi}{4} \phi^4 + \frac{\beta_\Phi}{8} \phi^4 \left( \ln \left[ \frac{\phi^2}{v_\phi^2} \right] - \frac{25}{6} \right), \quad (3.1)$$

where  $\phi/\sqrt{2} = \Re[\Phi]$ , and we have chosen the renormalization scale to be the VEV of  $\Phi$  ( $\langle \phi \rangle = v_\phi$ ). Here, the coefficient of the 1-loop quantum corrections is given by

$$\beta_\Phi = \frac{1}{16\pi^2} \left[ 20\lambda_\Phi^2 + 6x_\Phi^4 (g_{X1}^2 + g_X^2)^2 - 16 \sum_i (Y_M^i)^4 \right] \quad (3.2)$$

$$\simeq \frac{1}{16\pi^2} \left[ 6(x_\Phi g_X)^4 - 16 \sum_i (Y_M^i)^4 \right], \quad (3.3)$$

where in the last expression, we have used  $\lambda_\Phi^2 \ll (x_\Phi g_X)^4$  as usual in the Coleman-Weinberg mechanism and set  $g_{X1} = g_{1X} = 0$  at  $\langle \phi \rangle = v_\phi$ , for simplicity. The stationary condition

$dV/d\phi|_{\phi=v_\phi} = 0$  leads to

$$\lambda_\Phi = \frac{11}{6}\beta_\Phi, \quad (3.4)$$

and this  $\lambda_\Phi$  is nothing but a renormalized self-coupling at  $v_\phi$  defined as

$$\lambda_\Phi = \frac{1}{3!} \left. \frac{d^4 V(\phi)}{d\phi^4} \right|_{\phi=v_\phi}. \quad (3.5)$$

For more detailed discussion, see [5].

Associated with this radiative U(1)' symmetry breaking (as well as the electroweak symmetry breaking), the U(1)' gauge boson ( $Z'$  boson) and the right-handed Majorana neutrinos acquire their masses as

$$m_{Z'} = \sqrt{(x_\Phi g_X v_\phi)^2 + (x_H g_X v_h)^2} \simeq x_\Phi g_X v_\phi, \quad m_{N^i} = \sqrt{2} Y_M^i v_\phi, \quad (3.6)$$

where  $v_h = 246$  GeV is the SM Higgs VEV, and we have used  $x_\Phi v_\phi \gg x_H v_h$ , which will be verified below. In this paper, we assume degenerate masses for the three Majorana neutrinos,  $Y_M^i = y_M$  (equivalently,  $m_{N^i} = m_N$ ) for all  $i = 1, 2, 3$ , for simplicity. The U(1)' Higgs boson mass is given by

$$m_\phi^2 = \left. \frac{d^2 V}{d\phi^2} \right|_{\phi=v_\phi} = \beta_\Phi v_\phi^2 \simeq \frac{3}{8\pi^2} ((x_\Phi g_X)^4 - 8y_M^4) v_\phi^2 \simeq \frac{3}{8\pi^2} \frac{m_{Z'}^4 - 2m_N^4}{v_\phi^2}. \quad (3.7)$$

When the Yukawa coupling is negligibly small, this equation reduces to the well-known relation derived in the original paper by Coleman-Weinberg [2]. For a sizable Majorana mass, this formula indicates that the potential minimum disappears for  $m_N > m_{Z'}/2^{1/4}$ , so that there is an upper bound on the right-handed neutrino mass for the U(1)' symmetry to be broken radiatively. This is in fact the same reason as why the Coleman-Weinberg mechanism in the SM Higgs sector fails to break the electroweak symmetry when the top Yukawa coupling is large as observed. In order to avoid the destabilization of the U(1)' Higgs potential, we simply set  $m_{Z'}^4 \gg m_N^4$  in the following analysis. Note that this condition does not mean that the Majorana neutrinos must be very light, even though a factor difference between  $m_{Z'}$  and  $m_N$  is enough to satisfy the condition. For simplicity, we set  $y_M = 0$  at  $v_\phi$  in the following RG analysis.

## 4 Electroweak symmetry breaking

Let us now consider the SM Higgs sector. In our model, the electroweak symmetry breaking is achieved in a very simple way. Once the U(1)' symmetry is radiatively broken, the SM Higgs doublet mass is generated through the mixing quartic term between  $H$  and  $\Phi$  in the scalar potential in Eq. (2.5),

$$V(h) = \frac{\lambda_H}{4} h^4 + \frac{\lambda_{\text{mix}}}{4} v_\phi^2 h^2, \quad (4.1)$$



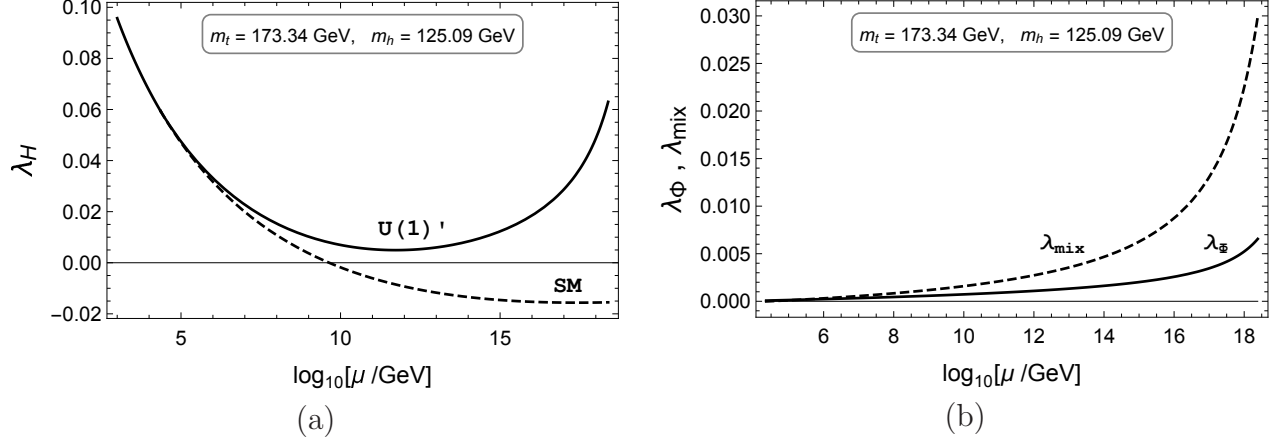


Figure 1: (a) The evolutions of the Higgs quartic coupling  $\lambda_H$  (solid line) for the inputs  $m_t = 173.34$  GeV and  $m_h = 125.09$  GeV, along with the SM case (dashed line). (b) The RG evolutions of  $\lambda_\Phi$  (solid line) and  $\lambda_{\text{mix}}$  (dashed line). Here, we have taken  $x_H = 2$ ,  $v_\phi = 23$  TeV and  $g_X(v_\phi) = 0.09$ .

where we have replaced  $H$  by  $H = 1/\sqrt{2}(0, h)$  in the unitary gauge. Choosing  $\lambda_{\text{mix}} < 0$ , the electroweak symmetry is broken in the same way as in the SM [6]. However, we should note that a crucial difference from the SM is that in our model the electroweak symmetry breaking originates from the radiative breaking of the  $U(1)'$  gauge symmetry. At the tree level, the stationary condition  $V'|_{h=v_h} = 0$  leads to the relation  $|\lambda_{\text{mix}}| = 2\lambda_H(v_h/v_\phi)^2$ , and the Higgs boson mass  $m_h$  is given by

$$m_h^2 = \left. \frac{d^2V}{dh^2} \right|_{h=v_h} = |\lambda_{\text{mix}}|v_\phi^2 = 2\lambda_H v_h^2. \quad (4.2)$$

In the following RG analysis, this is used as the boundary condition for  $\lambda_{\text{mix}}$  at the renormalization scale  $\mu = v_\phi$ . Note that since  $\lambda_H \sim 0.1$  and  $v_\phi \gtrsim 10$  TeV by the large electron-positron collider (LEP) constraint [14, 15, 16],  $|\lambda_{\text{mix}}| \lesssim 10^{-5}$ , which is very small.

In our discussion about the  $U(1)'$  symmetry breaking, we neglected  $\lambda_{\text{mix}}$  by assuming it to be negligibly small. Here we justify this treatment. In the presence of  $\lambda_{\text{mix}}$  and the Higgs VEV, Eq. (3.4) is modified as

$$\lambda_\Phi = \frac{11}{6}\beta_\Phi + \frac{|\lambda_{\text{mix}}|}{2} \left( \frac{v_h}{v_\phi} \right)^2 \simeq \frac{1}{2v_\phi^4} \left( \frac{11}{8\pi^2} m_{Z'}^4 + m_h^2 v_h^2 \right). \quad (4.3)$$

Considering the current LHC Run-2 bound from search for  $Z'$  boson resonances [17, 18],  $m_{Z'} \gtrsim 3$  TeV, we find that the first term in the parenthesis in the last equality is 5 orders of magnitude greater than the second term, and therefore we can analyze the two Higgs sectors separately.

## 5 Solving the SM Higgs vacuum instability

In the SM with the observed Higgs boson mass of  $m_h = 125.09$  GeV, the RG evolution of the SM Higgs quartic coupling shows that the running coupling becomes negative at the intermediate



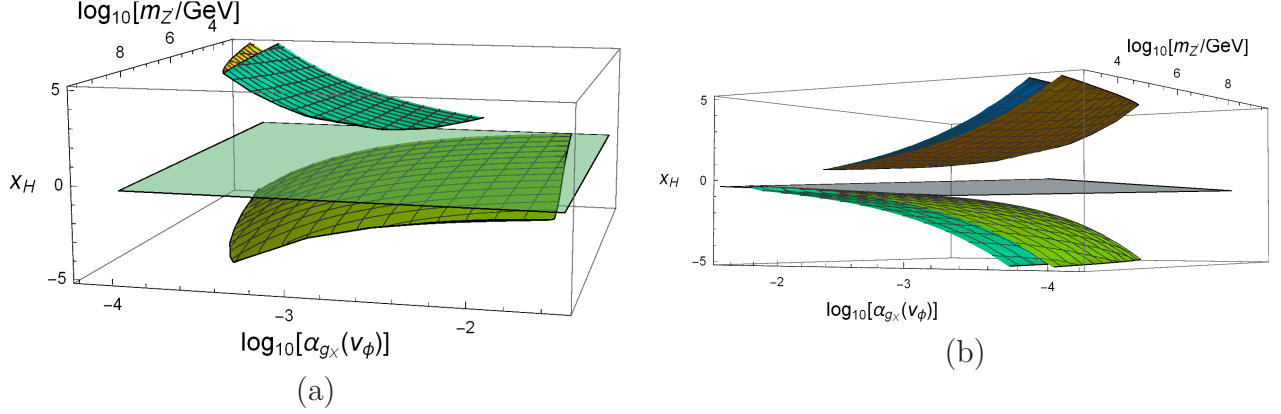


Figure 2: (a) The result of 3-dimensional parameter scans for  $v_\phi$ ,  $g_X$  and  $x_H$ , shown in  $(m_{Z'}, \alpha_{g_X}, x_H)$  parameter space with  $m_{Z'} \simeq x_\Phi g_X v_\phi$ , by using the inputs  $m_t = 173.34$  GeV and  $m_h = 125.09$  GeV. As a reference, a horizontal plane for  $x_H = -16/41$  is shown, which corresponds to the orthogonal case. (b) Same 3-dimensional parameter scans as (a), but deferent angle.

scale  $\mu \simeq 10^{10}$  GeV [11] for  $m_t = 173.34$  GeV, and hence the electroweak vacuum is unstable. In this section, we investigate RG evolution of the Higgs quartic coupling and a possibility to solve the Higgs vacuum instability problem in our  $U(1)'$  extended SM. Without the classical conformal invariance, Ref. [19] (see also [20]) has considered the same problem, and identified parameter regions which can resolve the Higgs vacuum instability. A crucial difference in our model is that because of the classical conformal invariance and the symmetry breaking by the Coleman-Weinberg mechanism, the initial values of  $\lambda_\Phi$  and  $\lambda_{\text{mix}}$  at  $v_\phi$  are not free parameters. Therefore, it is nontrivial to resolve the Higgs vacuum instability in the present model. The Higgs vacuum stability has been investigated in [5] for the classically conformal extension of the SM with an extend gauge groups and particle contents including a dark matter candidate.

In our RGE analysis, we employ the SM RGEs at the 2-loop level [11] from the top pole mass to the  $U(1)'$  Higgs VEV, and connect the RGEs to those of the  $U(1)'$  extended SM at the 2-loop level, which are generated by using SARAH [21]. RGEs used in our analysis are listed in Appendices. For inputs of the Higgs boson mass and top quark pole mass, we employ a central value of the ATLAS and CMS combined measurement  $m_h = 125.09$  GeV [10], while  $m_t = 173.34$  GeV is the central value of combined results of the Tevatron and the LHC measurements of top quark mass [12]. There are only 3 free parameters in our model, by which inputs at  $v_\phi$  are determined:  $x_H$ ,  $v_\phi$ , and  $g_X$ .

In Fig. 1 (a), we show the RG evolution of the SM Higgs quartic coupling in our model (solid line), along with the SM result (dashed line). Here, we have taken  $x_H = 2$ ,  $v_\phi = 23$  TeV, and  $g_X(v_\phi) = 0.09$  as an example. Recall that we have fixed  $x_\Phi = 2$  without loss of generality. The Higgs quartic coupling remains positive all the way up to the Planck mass, so that the Higgs vacuum instability problem is solved. There are complex, synergetic effects in the coupled RGEs to resolve the Higgs vacuum instability (see Appendices for RGEs). For example, the  $U(1)_Y$  gauge coupling grows faster than the SM case in the presence of the mixing gauge couplings  $g_{X1}$  and  $g_{1X}$ , which make the evolution of top Yukawa coupling decreasing faster than

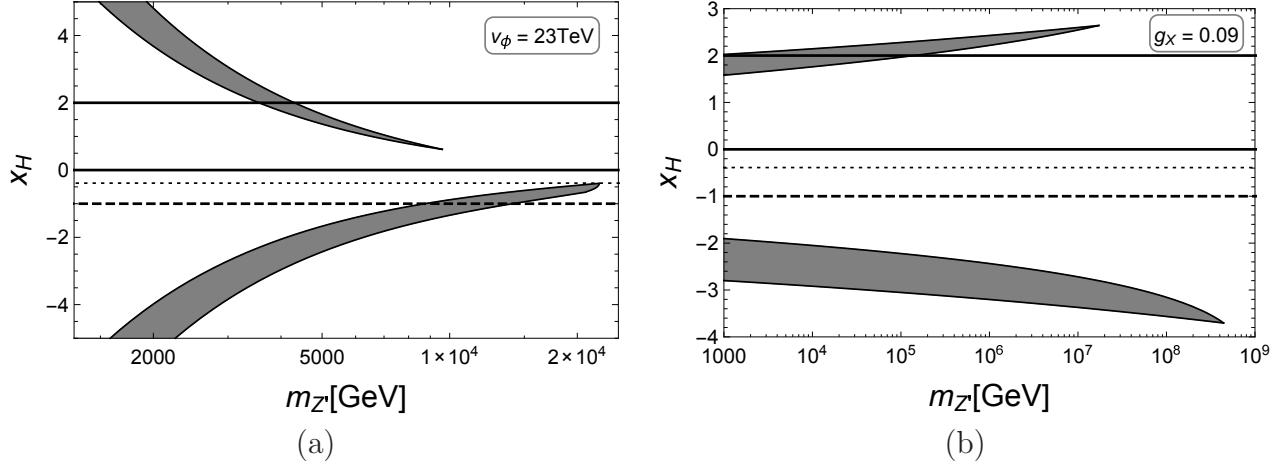


Figure 3: (a) The result of parameter scan for  $x_H$  and  $g_X$  with a fixed  $v_\phi = 23$  TeV, shown in  $(m_{Z'}, x_H)$ -plane with  $m_{Z'} \simeq x_\Phi g_X v_\phi$ . As a reference, horizontal lines are depicted for  $x_H = 2, 0$  [ $U(1)_{B-L}$  case],  $-16/41$  [orthogonal case], and  $-1$  [ $U(1)_R$  case]. (b) Same as (a), but parameter scan for  $x_H$  and  $v_\phi$  with a fixed  $g_X = 0.09$ .

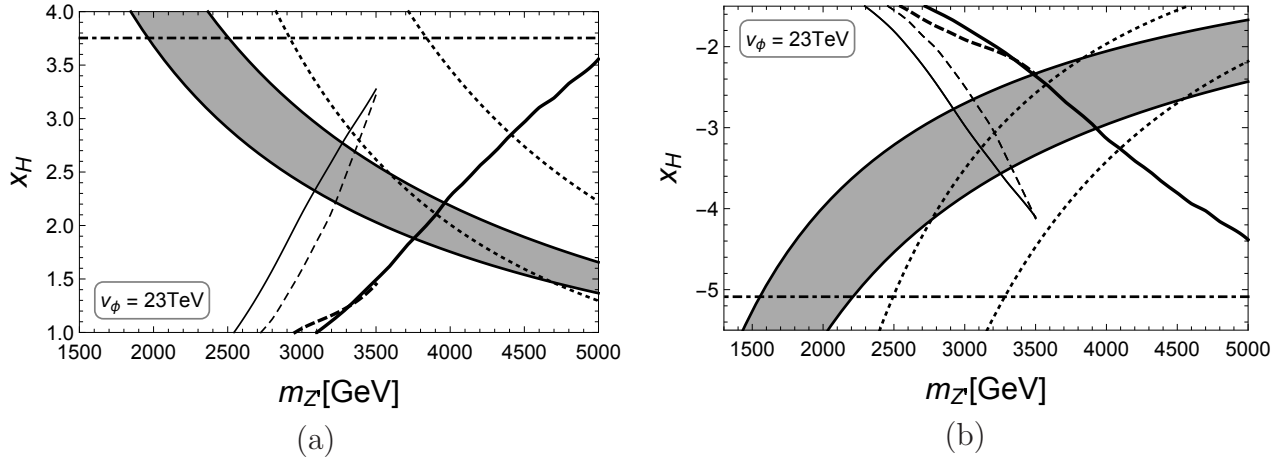


Figure 4: (a) The allowed positive  $x_H$  region at the TeV scale in Fig. 3 (a) is magnified, along with the LEP bound (dashed-dotted line), the LHC Run-1 CMS bound (thin dashed line), the LHC Run-1 ATLAS bound (thin solid line), the LHC Run-2 CMS bound (thick dashed line) and the LHC Run-2 ATLAS bound (thick solid line) from direct search for  $Z'$  boson resonance. The region on the left side of the lines are excluded. Here, the naturalness bounds for 10% (right dotted line) and 30% (left dotted line) fine-tuning levels are also depicted. (b) Same as (a), but for negative  $x_H$  region.

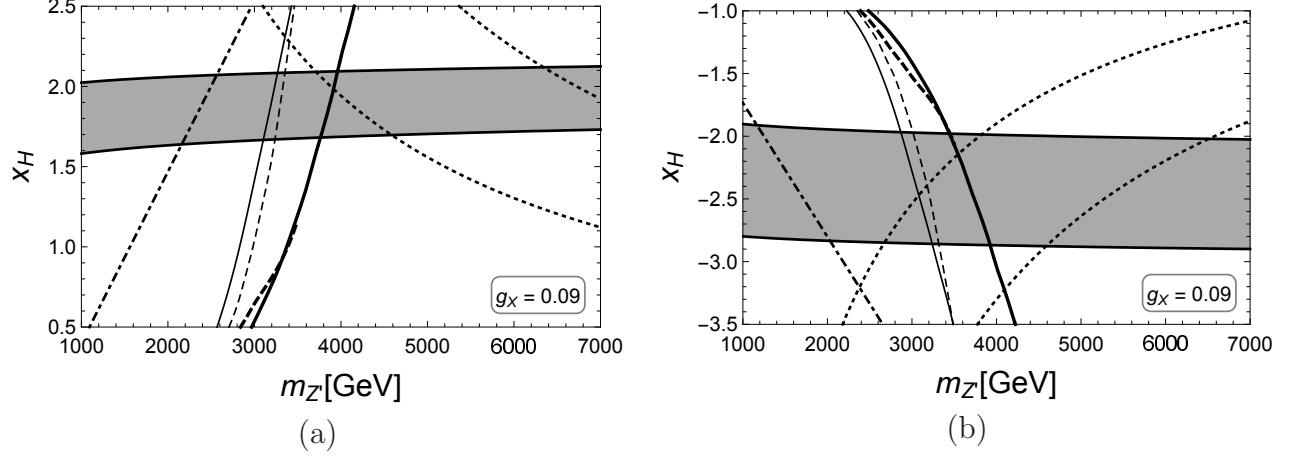


Figure 5: (a) Same as Fig. 4 (a), but magnifying Fig. 3 (b). (b) Same as Fig. 4 (b), but magnifying Fig. 3 (b).

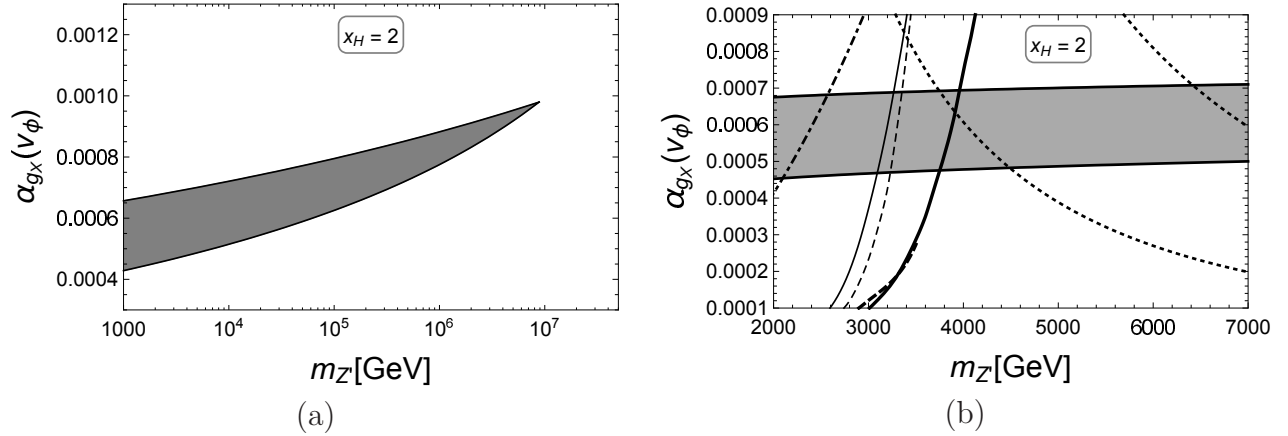


Figure 6: (a) The result of parameter scan for  $v_\phi$  and  $g_X$  with a fixed  $x_H = 2$  in  $(m_{Z'}, \alpha_{g_X})$ -plane. (b) The allowed region at the TeV scale in (a) is magnified, along with the LEP bound (dashed-dotted line), the LHC Run-1 CMS bound (thin dashed line), the LHC Run-1 ATLAS bound (thin solid line), the LHC Run-2 CMS bound (thick dashed line) and the LHC Run-2 ATLAS bound (thick solid line) from direct search for  $Z'$  boson resonance. The region on the left side of the lines are excluded. Here, the naturalness bounds for 10% (right dotted line) and 30% (left dotted line) fine-tuning levels are also depicted.

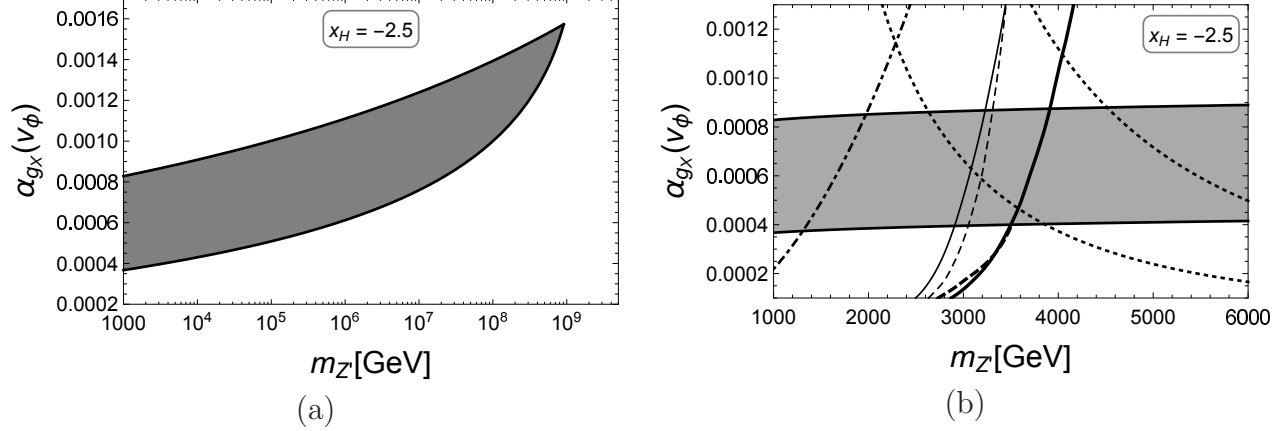


Figure 7: (a) Same as Fig. 6 (a), but for  $x_H = -2.5$ . (b) Same as Fig. 6 (b), but for  $x_H = -2.5$ .

in the SM case. The evolution of the mixing gauge coupling is controlled by the  $U(1)'$  gauge coupling. Both of them are asymptotic non-free. The gauge couplings positively contribute to the beta function of the SM Higgs quartic coupling, while the top Yukawa coupling gives a negative contribution. As a result, the RG evolutions of the gauge and top Yukawa couplings work to change the sign of the the beta function of the SM Higgs quartic coupling at  $\mu \simeq 10^{12}$  GeV in Fig. 1 (a). Figure 1 (b) shows the RG evolutions of the other Higgs quartic couplings. Note that the input of  $\lambda_\Phi$  and  $\lambda_{\text{mix}}$  are very small because of the radiative gauge symmetry breaking, and the two couplings remain very small even at the Planck mass. Thus, the positive contribution of  $\lambda_{\text{mix}}$  to the beta function of the SM Higgs quartic coupling is negligible. This is in sharp contrast to  $U(1)$  extended models without the conformal invariance, where  $\lambda_{\text{mix}}$  is a free parameter and we can take its input to give a large, positive contribution to the beta function, so that the Higgs vacuum instability problem is relatively easier to solve.

In order to identify a parameter region to resolve the Higgs vacuum instability, we perform parameter scans for the free parameters  $x_H$ ,  $v_\phi$  and  $g_X$ . In this analysis, we impose several conditions on the running couplings at  $v_\phi \leq \mu \leq M_P$  ( $M_P = 2.4 \times 10^{18}$  GeV is the reduced Planck mass): stability conditions of the Higgs potential ( $\lambda_H, \lambda_\Phi > 0$ ), the perturbative conditions that all the running couplings remain in the perturbative regime, namely,  $g_i^2$  ( $i = 1, 2, 3$ ),  $g_X^2$ ,  $g_{X1}^2$ ,  $g_{IX}^2 < 4\pi$  and  $\lambda_H, \lambda_\Phi, \lambda_{\text{mix}} < 4\pi$ . For theoretical consistency, we also impose a condition that the 2-loop beta functions are smaller than the 1-loop beta functions. In Fig. 2, we show the result of our parameter scans in the 3-dimensional parameter space of  $(m_{Z'}, \alpha_{g_X}, x_H)$ , where  $\alpha_{g_X} = g_X^2/(4\pi)$ . As a reference, we show a horizontal plane corresponding to the orthogonal case  $x_H = -16/41$ . There is no overlapping of the plane with the resultant parameter regions to resolve the electroweak vacuum instability.

In order to discuss our results in detail, we show in Figs. 3-7 the parameter scan results on several 2-dimensional hypersurfaces in the 3D plot of Fig. 2. In Fig. 3, our results are shown for  $x_H$  and  $g_X$  with a fixed  $v_\phi = 23$  TeV (a) and for  $x_H$  and  $v_\phi$  with a fixed  $g_X = 0.09$  (b) in  $(m_{Z'}, x_H)$ -plane, along with the horizontal lines corresponding to  $x_H = 2, 0$  [ $U(1)_{B-L}$  case],  $-16/41$  [orthogonal case], and  $-1$  [ $U(1)_R$  case]. We can see that the resultant parameter space is very restricted. For example, the Higgs vacuum instability can not be resolved in the classically conformal  $U(1)_{B-L}$  extended SM or the classically conformal orthogonal  $U(1)$

extended SM, for the inputs  $m_t = 173.34$  GeV and  $m_h = 125.09$  GeV. The allowed regions at the TeV scale in Figs. 3 (a) and 3 (b) are magnified in Fig. 4 and Fig. 5, respectively. Here we also show the collider bounds, namely the LEP bounds (dashed-dotted lines) [14, 15, 16], the CMS bounds at the LHC Run-1 (thin dashed lines) [22], the ATLAS bounds at the LHC Run-1 (thin solid lines) [23], the CMS bounds at the LHC Run-2 (thick dashed lines) [18], and the ATLAS bounds at the LHC Run-2 (thick solid lines) [17], from search for  $Z'$  boson mediated processes, which will be obtained in the next section. The region on the left side of the lines are excluded. Naturalness bounds (dotted lines), which will be obtained in Sec. 7, are also shown. These naturalness bounds for the 10% fine-tuning level are found to be compatible to the bounds obtained by the LHC Run-2 results. The result of parameter scan for  $v_\phi$  and  $\alpha_{g_X}$  with a fixed  $x_H = 2$  is depicted in Fig. 6 (a), and the allowed region at the TeV scale is magnified in Fig. 6 (b), along with the collider and naturalness bounds. Same plots as Fig. 6 but for  $x_H = -2.5$  are shown in Fig. 7.

## 6 LHC Run-2 bounds on the $U(1)'$ $Z'$ boson

The ATLAS and the CMS collaborations have searched for  $Z'$  boson resonance at the LHC Run-1 with  $\sqrt{s} = 8$  TeV, and continued the search at the LHC Run-2 with  $\sqrt{s} = 13$  TeV. The most stringent bounds on the  $Z'$  boson production cross section times branching ratio have been obtained by using the dilepton final state. For the so-called sequential SM  $Z'$  ( $Z'_{SSM}$ ) model [24], where the  $Z'_{SSM}$  boson has exactly the same couplings with the SM fermions as those of the SM  $Z$  boson, the cross section bounds from the LHC Run-1 results lead to lower bounds on the  $Z'_{SSM}$  boson mass as  $m_{Z'_{SSM}} \geq 2.90$  TeV from the ATLAS analysis [23] and  $m_{Z'_{SSM}} \geq 2.96$  TeV from the CMS analysis [22], respectively. Very recently, these bounds have been updated by the ATLAS [17] and CMS [18] analysis with the LHC Run-2 at  $\sqrt{s} = 13$  TeV as  $m_{Z'_{SSM}} \geq 3.4$  TeV (ATLAS) and  $m_{Z'_{SSM}} \geq 3.15$  TeV (CMS), respectively. We interpret theses ATLAS and CMS results to the  $U(1)'$   $Z'$  boson case, and derive an upper bound on  $x_H$  or  $\alpha_{g_X}$  as a function of  $m_{Z'}$ .

We calculate the dilepton production cross section for the process  $pp \rightarrow Z' + X \rightarrow \ell^+ \ell^- + X$ . The differential cross section with respect to the invariant mass  $M_{\ell\ell}$  of the final state dilepton is described as

$$\frac{d\sigma}{dM_{\ell\ell}} = \sum_{a,b} \int_{\frac{M_{\ell\ell}^2}{E_{CM}^2}}^1 dx_1 \frac{2M_{\ell\ell}}{x_1 E_{CM}^2} f_a(x_1, M_{\ell\ell}^2) f_b\left(\frac{M_{\ell\ell}^2}{x_1 E_{CM}^2}, M_{\ell\ell}^2\right) \hat{\sigma}(\bar{q}q \rightarrow Z' \rightarrow \ell^+ \ell^-), \quad (6.1)$$

where  $f_a$  is the parton distribution function for a parton “ $a$ ”, and  $E_{CM} = 13$  TeV (8 TeV) is the center-of-mass energy of the LHC Run-2 (Run-1). In our numerical analysis, we employ CTEQ5M [25] for the parton distribution functions. In the case of the  $U(1)'$  model, the cross section for the colliding partons with a fixed  $x_\Phi = 2$  is given by

$$\begin{aligned} \hat{\sigma}(\bar{u}u \rightarrow Z' \rightarrow \ell^+ \ell^-) &= \frac{\pi \alpha_{g_X}^2}{81} \frac{M_{\ell\ell}^2}{(M_{\ell\ell}^2 - m_{Z'}^2)^2 + m_{Z'}^2 \Gamma_{Z'}^2} (85x_H^4 + 152x_H^3 + 104x_H^2 + 32x_H + 4), \\ \hat{\sigma}(\bar{d}d \rightarrow Z' \rightarrow \ell^+ \ell^-) &= \frac{\pi \alpha_{g_X}^2}{81} \frac{M_{\ell\ell}^2}{(M_{\ell\ell}^2 - m_{Z'}^2)^2 + m_{Z'}^2 \Gamma_{Z'}^2} (25x_H^4 + 20x_H^3 + 8x_H^2 + 8x_H + 4), \end{aligned} \quad (6.2)$$

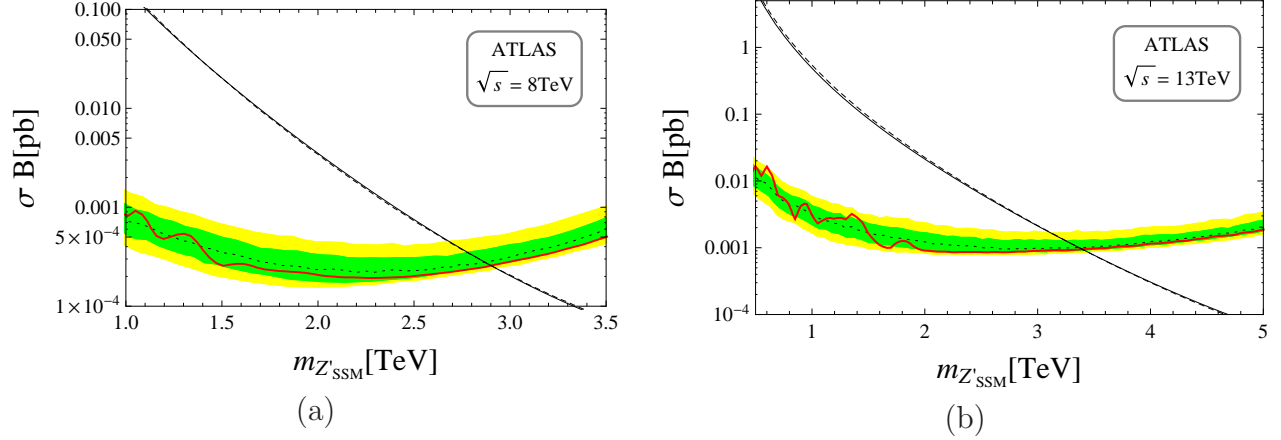


Figure 8: (a) The cross section as a function of the  $Z'_{SSM}$  mass (solid line) with  $k = 1.18$ , along with the LHC Run-1 ATLAS result from the combined dielectron and dimuon channels in Ref. [23]. (b) Same as (a), but with  $k = 1.19$ , along with the LHC Run-2 ATLAS result in Ref. [17].

where the total decay width of  $Z'$  boson is given by

$$\Gamma_{Z'} = \frac{\alpha_{g_X} m_{Z'}}{6} \left[ \frac{103x_H^2 + 86x_H + 37}{3} + \frac{17x_H^2 + 10x_H + 2 + (7x_H^2 + 20x_H + 4) \frac{m_t^2}{m_{Z'}^2}}{3} \sqrt{1 - \frac{4m_t^2}{m_{Z'}^2}} \right]. \quad (6.3)$$

Here, we have neglected all SM fermion masses except for  $m_t$ , and assumed  $m_N^i > m_{Z'}/2$  for simplicity. By integrating the differential cross section over a range of  $M_{\ell\ell}$  set by the ATLAS and the CMS analysis, respectively, we obtain the cross section as a function of  $x_H$ ,  $\alpha_{g_X}$  and  $m_{Z'}$ , which are compared with the lower bounds obtained by the ATLAS and the CMS collaborations.

In interpreting the ATLAS and the CMS results to the  $U(1)'$   $Z'$  boson, we follow the strategy in [26], where the minimal  $U(1)_{B-L}$  model has been investigated and an upper bound on the  $U(1)_{B-L}$  gauge coupling as a function of  $Z'$  boson mass has been obtained from the ATLAS and the CMS results at the LHC Run-2. We first analyze the sequential SM  $Z'$  model to check a consistency of our analysis with the one by the ATLAS and the CMS collaborations. With the same couplings as SM, we calculate the differential cross section of the process  $pp \rightarrow Z'_{SSM} + X \rightarrow \ell^+ \ell^- + X$  like Eq. (6.1). According to the analysis by the ATLAS collaboration at the LHC Run-1 (Run-2), we integrate the differential cross section for the range of  $128 \text{ GeV} \leq M_{\ell\ell} \leq 4500 \text{ GeV}$  [23] ( $128 \text{ GeV} \leq M_{\ell\ell} \leq 6000 \text{ GeV}$  [17]), and obtain the cross section of the dilepton production process as a function of  $Z'_{SSM}$  boson mass. Our results are shown as solid lines in Fig. 8 (a) for the LHC Run-1 and (b) for the LHC Run-2, respectively, along with the plots presented by the ATLAS collaborations at the LHC Run-1 [23] and the LHC Run-2 [17]. In Fig. 8 (a) and (b), the experimental upper bounds on the  $Z'$  boson production cross section are depicted as the horizontal solid (red) curves. The theoretical  $Z'$  boson production cross section are shown as the diagonal dashed lines, and the lower limits of the  $Z'_{SSM}$  boson

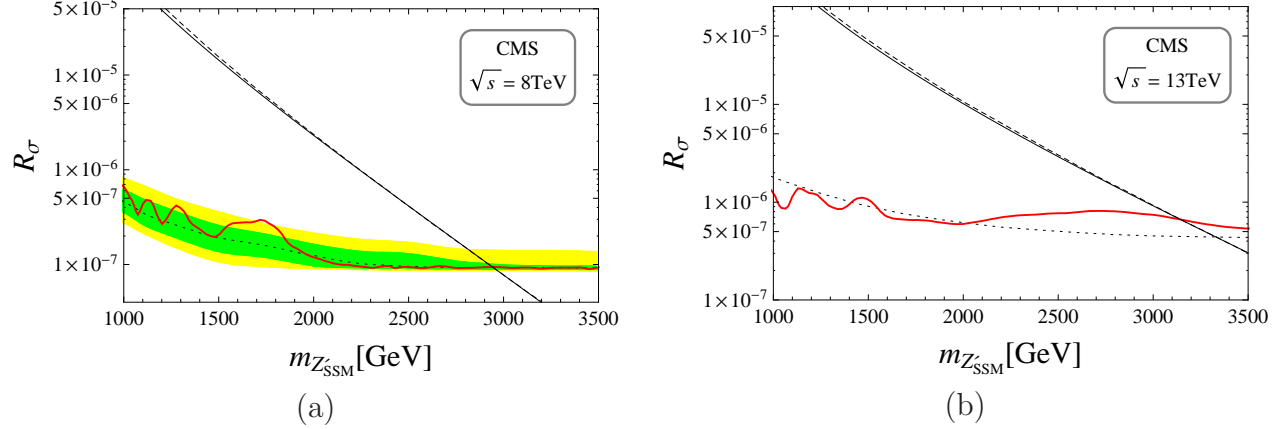


Figure 9: (a) The cross section ratio as a function of the  $Z'_{SSM}$  mass (solid line) with  $k = 1.01$ , along with the LHC Run-1 CMS result from the combined dielectron and dimuon channels in Ref. [22]. (b) Same as (a), but with  $k = 1.65$ , along with the LHC Run-2 CMS result in Ref. [18].

mass obtained by the ATLAS collaborations are found to be 2.90 TeV for the LHC Run-1 and 3.4 TeV for the LHC Run-2, respectively, which can be read off from the intersection points of the theoretical predictions (diagonal dashed lines) and the experimental cross section bounds (horizontal solid (red) curves). In order to take into account the difference of the parton distribution functions used in the ATLAS and our analysis and QCD corrections of the process, we have scaled our resultant cross sections by a factor  $k = 1.18$  in Fig. 8 (a) and by  $k = 1.19$  in Fig. 8 (b), with which we can obtain the same lower limits of the  $Z'_{SSM}$  boson mass as 2.90 TeV and 3.4 TeV. We can see that our results (solid lines) in Fig. 8 with the factors of  $k = 1.18$  and  $k = 1.19$ , respectively, are very consistent with the theoretical predictions (diagonal dashed lines) presented by the ATLAS collaborations. We use these factors in the following analysis for the  $U(1)' Z'$  production process.

Now we calculate the cross section of the process  $pp \rightarrow Z' + X \rightarrow \ell^+ \ell^- + X$  for various values of  $g_X$ ,  $x_H$  and  $v_\phi$ , and read off the constraints on these parameters from the cross section bounds given by the ATLAS collaborations. In Figs. 4-7, our results from the ATLAS bounds at the LHC Run-1 and Run-2 are depicted as thin solid lines and thick solid lines, respectively. We can see that the LHC Run-2 results have dramatically improved the bounds from those obtained by the LHC Run-1 results.

We apply the same strategy and compare our results for the  $Z'_{SSM}$  model with the those by the CMS Run-1 analysis [22] and the CMS Run-2 one [18]. According to the analysis by the CMS collaboration at the LHC Run-1 (Run-2), we integrate the differential cross section for the range of  $0.6 m_{Z'_{SSM}} \leq M_{\ell\ell} \leq 1.4 m_{Z'_{SSM}}$  [22] ( $0.97 m_{Z'_{SSM}} \leq M_{\ell\ell} \leq 1.03 m_{Z'_{SSM}}$  [18]) and obtain the cross section. In the CMS analysis, the limits are set on the ratio of the  $Z'_{SSM}$  boson cross section to the  $Z/\gamma^*$  cross section:

$$R_\sigma = \frac{\sigma(pp \rightarrow Z' + X \rightarrow \ell\ell + X)}{\sigma(pp \rightarrow Z + X \rightarrow \ell\ell + X)}, \quad (6.4)$$

where the  $Z/\gamma^*$  production cross section in the mass window of  $60 \text{ GeV} \leq M_{\ell\ell} \leq 120 \text{ GeV}$  are



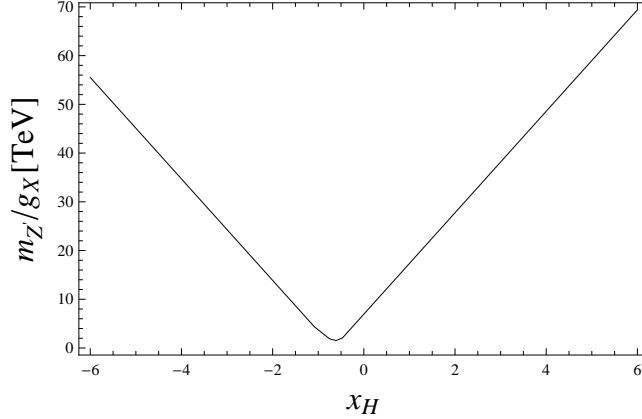


Figure 10: The lower bound on  $m_{Z'}/g_X$  as a function  $x_H$  (with a fixed  $x_\phi=2$ ), obtained by the limits from the final LEP 2 data [16] at 95% confidence level.

predicted to be 1117 pb at the LHC Run-1 [22] and 1928 pb at the LHC Run-2 [18], respectively. Our results for the  $Z'_{SSM}$  model are shown as the solid lines in Fig. 9 (a) and (b), along with the plots presented in [22] and [18], respectively. The analyses in these CMS papers lead to the lower limits of the  $Z'_{SSM}$  boson mass as 2.96 TeV for the LHC Run-1 and 3.15 TeV for the LHC Run-2, which are read off from the intersection points of the theoretical predictions (diagonal dashed lines) and the experimental cross section bounds (horizontal solid (red) curves). In order to obtain the same lower mass limits, we have scaled our resultant cross sections by a factor  $k = 1.01$  in Fig. 9 (a) and by  $k = 1.65$  in Fig. 9 (b), respectively. With these  $k$  factors, our results (solid lines) are very consistent with the theoretical predictions (diagonal dashed lines) presented in Refs. [22] and [18]. We use these  $k$  factors in our analysis to interpret the CMS results to the  $U(1)'$   $Z'$  boson case. In Figs. 4-7, our results from the CMS bounds at the LHC Run-1 and Run-2 are depicted as thin dashed lines and thick dashed lines, respectively. We can see that the CMS results at the LHC Run-2 have dramatically improved the bounds obtained by the LHC Run-1 results. We find that the ATLAS and the CMS bounds we have obtained are consistent with each other. For the LHC Run-2 results, the ATLAS bounds are slightly more severe than the CMS bounds for  $m_{Z'} \leq 3.5$  TeV, and applicable up to  $m_{Z'} = 5$  TeV, leading to the most severe LHC bound on the model parameters.

The search for effective 4-Fermi interactions mediated by the  $Z'$  boson at the LEP leads to a lower bound on  $m_{Z'}/g_X$  [14, 15, 16]. Employing the limits from the final LEP 2 data [16] at 95% confidence level, we follow [15] and derive a lower bound on  $m_{Z'}/g_X$  as a function  $x_H$ . Our result is shown in Fig. 10. In Figs. 4-7, the LEP bounds are depicted as the dashed-dotted lines.

## 7 Naturalness bounds from SM Higgs mass corrections

Once the classical conformal symmetry is radiatively broken by the Coleman-Weinberg mechanism, the masses for the  $Z'$  boson and the Majorana neutrinos are generated and they contribute

to self-energy corrections of the SM Higgs doublet. If the  $U(1)'$  gauge symmetry breaking scale is very large, the self-energy corrections may exceed the electroweak scale and require us to fine-tune the model parameters in reproducing the correct electroweak scale. See [27] for related discussions. We consider two heavy states, the right-handed neutrino and  $Z'$  boson, whose masses are generated by the  $U(1)'$  gauge symmetry breaking.

Since the original theory is classically conformal and defined as a massless theory, the self-energy corrections to the SM Higgs doublet originates from corrections to the mixing quartic coupling  $\lambda_{\text{mix}}$ . Thus, what we calculate to derive the naturalness bounds is quantum corrections to the term  $\lambda_{\text{mix}} h^2 \phi^2$  in the effective Higgs potential

$$V_{\text{eff}} \supset \frac{\lambda_{\text{mix}}}{4} h^2 \phi^2 + \frac{\beta_{\lambda_{\text{mix}}}}{8} h^2 \phi^2 (\ln [\phi^2] + C), \quad (7.1)$$

where the logarithmic divergence and the terms independent of  $\phi$  are all encoded in  $C$ . Here, the major contributions to quantum corrections are found to be

$$\beta_{\lambda_{\text{mix}}} \supset -\frac{48|y_M|^2|Y_\nu|^2}{16\pi^2} + \frac{12x_H^2 x_\Phi^2 g_X^4}{16\pi^2} - \frac{4(19x_H^2 + 10x_H x_\Phi + x_\Phi^2) x_\Phi^2 y_t^2 g_X^4}{(16\pi^2)^2}, \quad (7.2)$$

where the first term comes from the one-loop diagram involving the Majorana neutrinos, the second one is from the one-loop diagram involving the  $Z'$  boson, and the third one is from the two-loop diagram [6] involving the  $Z'$  boson and the top quark. By adding a counter term, we renormalize the coupling  $\lambda_{\text{mix}}$  with the renormalization condition,

$$\left. \frac{\partial^4 V_{\text{eff}}}{\partial h^2 \partial \phi^2} \right|_{h=0, \phi=v_\phi} = \lambda_{\text{mix}}, \quad (7.3)$$

where  $\lambda_{\text{mix}}$  is the renormalized coupling. As a result, we obtain

$$V_{\text{eff}} \supset \frac{\lambda_{\text{mix}}}{4} h^2 \phi^2 + \frac{\beta_{\lambda_{\text{mix}}}}{8} h^2 \phi^2 \left( \ln \left[ \frac{\phi^2}{v_\phi^2} \right] - 3 \right). \quad (7.4)$$

Substituting  $\phi = v_\phi$ , we obtain the SM Higgs self-energy correction as

$$\begin{aligned} \Delta m_h^2 &= -\frac{3}{4} \beta_{\lambda_{\text{mix}}} v_\phi^2 \\ &\sim \frac{9m_\nu m_N^3}{4\pi^2 v_h^2} - \frac{9}{4\pi} x_H^2 \alpha_{g_X} m_{Z'}^2 + \frac{3m_t^2}{32\pi^3 v_h^2} (19x_H^2 + 20x_H + 4) \alpha_{g_X} m_{Z'}^2, \end{aligned} \quad (7.5)$$

where we have used the seesaw formula,  $m_\nu \sim Y_\nu^2 v_h^2 / 2m_N$  [9], and set  $x_\Phi = 2$ . For the stability of the electroweak vacuum, we impose  $\Delta m_h^2 \lesssim m_h^2$  as the naturalness. For example, when the light neutrino mass scale is around  $m_\nu \sim 0.1$  eV, we have an upper bound from the first term of Eq. (7.5) for the Majorana mass as  $m_N \lesssim 3 \times 10^6$  GeV. This bound is much larger than the scale that we are interested in,  $m_N \lesssim 1$  TeV. The most important contribution to  $\Delta m_h^2$  is the second term of Eq. (7.5) generated through the one-loop diagram with the  $Z'$  gauge boson, and the third term becomes important in the case of  $U(1)_{B-L}$  model, because  $x_H = 0$  condition makes the second term vanished.

If  $\Delta m_h^2$  is much larger than the electroweak scale, we need a fine-tuning of the tree-level Higgs mass ( $|\lambda_{\text{mix}}|v_\phi^2/2$ ) to reproduce the correct SM Higgs VEV,  $v_h = 246$  GeV. We simply evaluate a fine-tuning level as

$$\delta = \frac{m_h^2}{2|\Delta m_h^2|}. \quad (7.6)$$

Here,  $\delta = 0.1$ , for example, indicates that we need to fine-tune the tree-level Higgs mass squared at the accuracy of 10% level. In Figs. 4-7, the naturalness bounds for 10% and 30% fine-tuning levels are plotted as the dotted lines. Interestingly, the naturalness bounds from the 30% fine-tuning level are found to be compatible to the ATLAS bounds from the LHC Run-2.

## 8 Conclusions

We have considered the classically conformal  $U(1)'$  extended SM with three right-handed neutrinos and a  $U(1)'$  Higgs singlet field. The  $U(1)'$  symmetry is radiatively broken by the Coleman-Weinberg mechanism, by which the  $Z'$  boson as well as the right-handed (Majorana) neutrinos acquire their masses. With the Majorana heavy neutrinos, the seesaw mechanism is automatically implemented. Through a mixing quartic term between the  $U(1)'$  Higgs and the SM Higgs doublet fields, a negative mass squared for the SM Higgs doublet is generated and, as a result, the electroweak symmetry breaking is triggered associated with the radiative  $U(1)'$  gauge symmetry breaking. Therefore, all mass generations occur through the dimensional transmutation in our model.

In the context of the classically conformal  $U(1)'$  model, we have investigated a possibility to resolve the electroweak vacuum instability. Since the gauge symmetry is broken by the Coleman-Weinberg mechanism, all quartic couplings in the Higgs potential except the SM Higgs one are very small, and hence their positive contributions to the  $U(1)'$  model are not effective in resolving the SM Higgs vacuum instability. On the other hand, in the  $U(1)'$  model, the SM Higgs doublet has a nonzero  $U(1)'$  charge, and this gauge interaction positively contributes to the beta function. In addition, the  $U(1)'$  gauge interaction negatively contributes to the beta function of the top Yukawa coupling, so that the running top Yukawa coupling is decreasing faster than in the SM case, and its negative contribution to the beta function of the SM Higgs quartic coupling becomes milder. For three free parameters of the model,  $m_{Z'}$ ,  $\alpha_{g_X}$  and  $x_H$ , we have performed parameter scan by analyzing the renormalization group evolutions of the model parameters at the two-loop level, and identified parameter regions which can solve the electroweak vacuum instability problem and keep all coupling values in perturbative regime up to the Planck mass. We have found that the resultant parameter regions are very severely constrained, and also that the  $U(1)_{B-L}$  model and the orthogonal model are excluded from having the electroweak vacuum stability with the current world average of the experimental data,  $m_t = 173.34$  GeV [12] and  $m_h = 125.09$  GeV [10].

We have also considered the current collider bounds on the  $U(1)'$   $Z'$  boson mass from the recent ATLAS and CMS results at the LHC Run-2 with  $\sqrt{s} = 13$  TeV. We have interpreted the  $Z'$  boson resonance search results at the LHC Run-1 and Run-2 to the  $U(1)'$   $Z'$  boson case, and obtained the collider bound on the  $U(1)'$  charge of the SM Higgs doublet  $x_H$  for a fixed

U(1)' gauge coupling, the collider bound on  $x_H$  for a fixed VEV of the U(1)' Higgs, or the upper bound on the the U(1)' gauge coupling for a fixed  $x_H$  as a function of the U(1)'  $Z'$  boson mass  $m_{Z'}$ . The LEP results on search for effective 4-Fermi interactions mediated by the U(1)'  $Z'$  boson can also constrain the model parameter space, but the constraint is found to be weaker than those obtained from the LHC Run-2 results.

Once the U(1)' gauge symmetry is broken, the  $Z'$  boson and the right-handed neutrinos become heavy, and contribute to the SM Higgs self-energy through quantum corrections. Therefore, the SM Higgs self-energy can exceed the electroweak scale, if the states are so heavy. Since the SM Higgs doublet has nonzero U(1)' charge, the self-energy corrections from  $Z'$  boson occur at the one loop level. This is in sharp contrast with the classically conformal U(1)<sub>B-L</sub> model [6], where the Higgs doublet has no U(1)<sub>B-L</sub> charge, and the self-energy corrections from  $Z'$  boson occur at the two-loop level. We have evaluated the Higgs self-energy corrections and found the naturalness bounds to reproduce the right electroweak scale for the fine-tuning level better than 10%. We have found that the naturalness bounds for the 30% fine-tuning level is compatible to the ATLAS constraint from the LHC Run-2 results, and requiring the fine-tuning level  $> 10\%$  leads to the upper bound on the U(1)'  $Z'$  boson mass as  $m_{Z'} \lesssim 7$  TeV.

Putting all our results together in Figs. 4-7, we have found that the U(1)'  $Z'$  boson mass lies in the range of  $3.5 \text{ TeV} \lesssim m_{Z'} \lesssim 7 \text{ TeV}$ . This region can be explored by the LHC Run-2 in the near future.

## Acknowledgments

The work of D.T. and S.O. were supported by the Sugawara unit and Hikami unit, respectively, of the Okinawa Institute of Science and Technology Graduate University. The work of N.O. was supported in part by the United States Department of Energy (DE-SC0013680).

## A THE U(1)' RGEs AT TWO-LOOP LEVEL

In this appendix we present the two-loop RGEs for the U(1)' extension of the SM, which are used in our analysis. The definitions of the covariant derivative, the Yukawa interactions and the scalar potential are given by Eqs. (2.1), (2.3) and (2.5), respectively. We only include the top quark Yukawa coupling  $y_t$  and the right-handed neutrino Majorana Yukawa coupling  $y_M = Y_M^i$  ( $i = 1, 2, 3$ ), since the other Yukawa couplings are negligibly small. The U(1)' charges  $x_i$  are defined in Table 1. The U(1)' RGEs at the two-loop level have been generated by using SARAH [21].

### A.1 The U(1)' RGEs for the gauge couplings

The RGEs for the gauge couplings at the two-loop level are given by

$$\mu \frac{dg_i}{d\mu} = \beta_{g_i}^{(1)} + \beta_{g_i}^{(2)}, \quad (\text{A.1})$$

where  $\beta_{g_i}^{(1)}$  and  $\beta_{g_i}^{(2)}$  are the one-loop and two-loop beta functions for the gauge couplings, respectively, and  $g_i$  represents  $g_3, g_2, g_1, g_{X1}, g_{1X}$  and  $g_X$ . Here, the one-loop beta functions for the gauge couplings are given by

$$\begin{aligned}
\beta_{g_3}^{(1)} &= \frac{g_3^3}{16\pi^2} \left[ -7 \right], \\
\beta_{g_2}^{(1)} &= \frac{g_2^3}{16\pi^2} \left[ -\frac{19}{6} \right], \\
\beta_{g_1}^{(1)} &= \frac{1}{16\pi^2} \left[ g_1 \left\{ \frac{41}{6} g_1^2 + \frac{1}{3} (82x_H + 16x_\Phi) g_1 g_{X1} + \frac{1}{3} (82x_H^2 + 32x_H x_\Phi + 9x_\Phi^2) g_{X1}^2 \right\} \right. \\
&\quad + g_{1X} \left\{ \frac{41}{6} g_1 g_{1X} + \frac{1}{3} (41x_H + 8x_\Phi) g_1 g_X + \frac{1}{3} (41x_H + 8x_\Phi) g_{1X} g_{X1} \right. \\
&\quad \left. \left. + \frac{1}{3} (82x_H^2 + 32x_H x_\Phi + 9x_\Phi^2) g_{X1} g_X \right\} \right], \\
\beta_{g_{X1}}^{(1)} &= \frac{1}{16\pi^2} \left[ g_{X1} \left\{ \frac{41}{6} g_1^2 + \frac{1}{3} (82x_H + 16x_\Phi) g_1 g_{X1} + \frac{1}{3} (82x_H^2 + 32x_H x_\Phi + 9x_\Phi^2) g_{X1}^2 \right\} \right. \\
&\quad + g_X \left\{ \frac{41}{6} g_1 g_{1X} + \frac{1}{3} (41x_H + 8x_\Phi) g_1 g_X + \frac{1}{3} (41x_H + 8x_\Phi) g_{1X} g_{X1} \right. \\
&\quad \left. \left. + \frac{1}{3} (82x_H^2 + 32x_H x_\Phi + 9x_\Phi^2) g_{X1} g_X \right\} \right], \\
\beta_{g_{1X}}^{(1)} &= \frac{1}{16\pi^2} \left[ g_{1X} \left\{ \frac{41}{6} g_{1X}^2 + \frac{1}{3} (82x_H + 16x_\Phi) g_{1X} g_X + \frac{1}{3} (82x_H^2 + 32x_H x_\Phi + 9x_\Phi^2) g_X^2 \right\} \right. \\
&\quad + g_1 \left\{ \frac{41}{6} g_1 g_{1X} + \frac{1}{3} (41x_H + 8x_\Phi) g_1 g_X + \frac{1}{3} (41x_H + 8x_\Phi) g_{1X} g_{X1} \right. \\
&\quad \left. \left. + \frac{1}{3} (82x_H^2 + 32x_H x_\Phi + 9x_\Phi^2) g_{X1} g_X \right\} \right], \\
\beta_{g_X}^{(1)} &= \frac{1}{16\pi^2} \left[ g_X \left\{ \frac{41}{6} g_{1X}^2 + \frac{1}{3} (82x_H + 16x_\Phi) g_{1X} g_X + \frac{1}{3} (82x_H^2 + 32x_H x_\Phi + 9x_\Phi^2) g_X^2 \right\} \right. \\
&\quad + g_{X1} \left\{ \frac{41}{6} g_1 g_{1X} + \frac{1}{3} (41x_H + 8x_\Phi) g_1 g_X + \frac{1}{3} (41x_H + 8x_\Phi) g_{1X} g_{X1} \right. \\
&\quad \left. \left. + \frac{1}{3} (82x_H^2 + 32x_H x_\Phi + 9x_\Phi^2) g_{X1} g_X \right\} \right], \tag{A.2}
\end{aligned}$$

and the two-loop beta functions for the gauge couplings are given by

$$\begin{aligned}
\beta_{g_3}^{(2)} &= \frac{1}{(16\pi^2)^2} \cdot \frac{g_3^3}{6} \left[ 11g_1^2 + 27g_2^2 - 156g_3^2 + 11g_{1X}^2 + 44g_{1X}g_Xx_H + 44g_1g_{X1}x_H + 44g_X^2x_H^2 \right. \\
&\quad \left. + 44g_{X1}^2x_H^2 + 4g_{1X}g_Xx_\Phi + 4g_1g_{X1}x_\Phi + 8g_X^2x_Hx_\Phi + 8g_{X1}^2x_Hx_\Phi + 2g_X^2x_\Phi^2 + 2g_{X1}^2x_\Phi^2 - 12y_t^2 \right], \\
\beta_{g_2}^{(2)} &= \frac{1}{(16\pi^2)^2} \cdot \frac{g_2^3}{6} \left[ 9g_1^2 + 35g_2^2 + 72g_3^2 + 9g_{1X}^2 + 36g_{1X}g_Xx_H + 36g_1g_{X1}x_H + 36g_X^2x_H^2 + 36g_{X1}^2x_H^2 \right. \\
&\quad \left. + 12g_{1X}g_Xx_\Phi + 12g_1g_{X1}x_\Phi + 24g_X^2x_Hx_\Phi + 24g_{X1}^2x_Hx_\Phi + 6g_X^2x_\Phi^2 + 6g_{X1}^2x_\Phi^2 - 9y_t^2 \right], \\
\beta_{g_1}^{(2)} &= \frac{1}{(16\pi^2)^2} \cdot \frac{1}{18} \left[ 199g_1^5 + 81g_1^3g_2^2 + 264g_1^3g_3^2 + 398g_1^3g_{1X}^2 + 81g_1g_2^2g_{1X}^2 + 264g_1g_3^2g_{1X}^2 \right. \\
&\quad + 199g_1g_{1X}^4 + 1194g_1^3g_{1X}g_Xx_H + 162g_1g_2^2g_{1X}g_Xx_H + 528g_1g_3^2g_{1X}g_Xx_H \\
&\quad + 1194g_1g_{1X}^3g_Xx_H + 1592g_1^4g_{X1}x_H + 324g_1^2g_2^2g_{X1}x_H + 1056g_1^2g_3^2g_{X1}x_H + 1990g_1^2g_{1X}^2g_{X1}x_H \\
&\quad + 162g_2^2g_{1X}^2g_{X1}x_H + 528g_3^2g_{1X}^2g_{X1}x_H + 398g_{1X}^4g_{X1}x_H + 796g_1^3g_X^2x_H^2 + 2388g_1g_{1X}^2g_X^2x_H^2 \\
&\quad + 5572g_1^2g_{1X}g_Xg_{X1}x_H^2 + 324g_2^2g_{1X}g_Xg_{X1}x_H^2 + 1056g_3^2g_{1X}g_Xg_{X1}x_H^2 + 2388g_{1X}^3g_Xg_{X1}x_H^2 \\
&\quad + 4776g_1^3g_{X1}^2x_H^2 + 324g_1g_2^2g_{X1}^2x_H^2 + 1056g_1g_3^2g_{X1}^2x_H^2 + 3184g_1g_{1X}^2g_{X1}^2x_H^2 + 1592g_1g_{1X}g_{X1}^3x_H^3 \\
&\quad + 3184g_1^2g_X^2g_{X1}x_H^3 + 4776g_{1X}^2g_X^2g_{X1}x_H^3 + 7960g_1g_{1X}g_Xg_{X1}^2x_H^3 + 6368g_1^2g_{X1}^3x_H^3 \\
&\quad + 1592g_{1X}^2g_{X1}^3x_H^3 + 3184g_{1X}g_X^3g_{X1}x_H^4 + 3184g_1g_X^2g_{X1}^2x_H^4 + 3184g_{1X}g_Xg_{X1}^3x_H^4 \\
&\quad + 3184g_1g_{X1}^4x_H^4 + 246g_1^3g_{1X}g_Xx_\Phi + 54g_1g_2^2g_{1X}g_Xx_\Phi + 48g_1g_3^2g_{1X}g_Xx_\Phi \\
&\quad + 246g_1g_{1X}^3g_Xx_\Phi + 328g_1^4g_{X1}x_\Phi + 108g_1^2g_2^2g_{X1}x_\Phi + 96g_1^2g_3^2g_{X1}x_\Phi + 410g_1^2g_{1X}^2g_{X1}x_\Phi \\
&\quad + 54g_2^2g_{1X}^2g_{X1}x_\Phi + 48g_3^2g_{1X}^2g_{X1}x_\Phi + 82g_{1X}^4g_{X1}x_\Phi + 328g_1^3g_X^2x_Hx_\Phi + 984g_1g_{1X}^2g_X^2x_Hx_\Phi \\
&\quad + 2296g_1^2g_{1X}g_Xg_{X1}x_Hx_\Phi + 216g_2^2g_{1X}g_Xg_{X1}x_Hx_\Phi + 192g_3^2g_{1X}g_Xg_{X1}x_Hx_\Phi \\
&\quad + 984g_{1X}^3g_Xg_{X1}x_Hx_\Phi + 1968g_1^3g_{X1}^2x_Hx_\Phi + 216g_1g_2^2g_{X1}^2x_Hx_\Phi + 192g_1g_3^2g_{X1}^2x_Hx_\Phi \\
&\quad + 1312g_1g_{1X}^2g_{X1}^2x_Hx_\Phi + 984g_1g_{1X}g_X^3x_H^2x_\Phi + 1968g_1^2g_X^2g_{X1}x_H^2x_\Phi + 2952g_{1X}^2g_X^2g_{X1}x_H^2x_\Phi \\
&\quad + 4920g_1g_{1X}g_Xg_{X1}^2x_H^2x_\Phi + 3936g_1^2g_{X1}^2x_H^2x_\Phi + 984g_{1X}^2g_{X1}^2x_H^2x_\Phi + 2624g_{1X}g_X^3g_{X1}x_H^3x_\Phi \\
&\quad + 2624g_1g_X^2g_{X1}^2x_H^3x_\Phi + 2624g_{1X}g_Xg_{X1}^3x_H^3x_\Phi + 2624g_1g_{X1}^4x_H^3x_\Phi + 46g_1^3g_X^2x_\Phi^2 \\
&\quad + 138g_1g_{1X}^2g_X^2x_\Phi^2 + 322g_1^2g_{1X}g_Xg_{X1}x_\Phi^2 + 54g_2^2g_{1X}g_Xg_{X1}x_\Phi^2 + 48g_3^2g_{1X}g_Xg_{X1}x_\Phi^2 \\
&\quad + 138g_{1X}^3g_Xg_{X1}x_\Phi^2 + 276g_1^3g_{X1}^2x_\Phi^2 + 54g_1g_2^2g_{X1}^2x_\Phi^2 + 48g_1g_3^2g_{X1}^2x_\Phi^2 + 184g_1g_{1X}^2g_{X1}^2x_\Phi^2 \\
&\quad + 276g_1g_{1X}g_X^3x_Hx_\Phi^2 + 552g_1^2g_X^2g_{X1}x_Hx_\Phi^2 + 828g_{1X}^2g_X^2g_{X1}x_Hx_\Phi^2 + 1380g_1g_{1X}g_Xg_{X1}^2x_Hx_\Phi^2 \\
&\quad + 1104g_1^2g_{X1}^3x_Hx_\Phi^2 + 276g_{1X}^2g_{X1}^3x_Hx_\Phi^2 + 1104g_{1X}g_X^3g_{X1}x_H^2x_\Phi^2 + 1104g_1g_X^2g_{X1}^2x_H^2x_\Phi^2 \\
&\quad + 1104g_{1X}g_Xg_{X1}^2x_H^2x_\Phi^2 + 1104g_1g_{X1}^4x_H^2x_\Phi^2 + 28g_1g_{1X}g_X^3x_\Phi^3 + 56g_1^2g_X^2g_{X1}x_\Phi^3 \\
&\quad + 84g_{1X}^2g_X^2g_{X1}x_\Phi^3 + 140g_1g_{1X}g_Xg_{X1}^2x_\Phi^3 + 112g_1^2g_{X1}^3x_\Phi^3 + 28g_{1X}^2g_{X1}^3x_\Phi^3 + 224g_{1X}g_X^3g_{X1}x_Hx_\Phi^3 \\
&\quad + 224g_1g_X^2g_{X1}^2x_Hx_\Phi^3 + 224g_{1X}g_Xg_{X1}^3x_Hx_\Phi^3 + 224g_1g_{X1}^4x_Hx_\Phi^3 + 100g_{1X}g_X^3g_{X1}x_\Phi^4 \\
&\quad + 100g_1g_X^2g_{X1}^2x_\Phi^4 + 100g_{1X}g_Xg_{X1}^2x_\Phi^4 + 100g_1g_{X1}^4x_\Phi^4 - 54g_{1X}g_Xg_{X1}^2y_M^2 - 54g_1g_{X1}^2x_\Phi^2y_M^2 \\
&\quad - 51g_1^3y_t^2 - 51g_1g_{1X}^2y_t^2 - 102g_1g_{1X}g_Xx_Hy_t^2 - 204g_1^2g_{X1}x_Hy_t^2 - 102g_{1X}^2g_{X1}x_Hy_t^2 \\
&\quad - 204g_{1X}g_Xg_{X1}^2x_Hy_t^2 - 204g_1g_{X1}^2x_Hy_t^2 - 15g_1g_{1X}g_Xx_\Phi y_t^2 - 30g_1^2g_{X1}x_\Phi y_t^2 \\
&\quad \left. - 15g_{1X}^2g_{X1}x_\Phi y_t^2 - 60g_{1X}g_Xg_{X1}x_Hx_\Phi y_t^2 - 60g_1g_{X1}^2x_Hx_\Phi y_t^2 - 6g_{1X}g_Xg_{X1}x_\Phi^2y_t^2 - 6g_1g_{X1}^2x_\Phi^2y_t^2 \right],
\end{aligned}$$

$$\begin{aligned}
\beta_{g_{X1}}^{(2)} = & \frac{1}{(16\pi^2)^2} \cdot \frac{1}{18} \left[ 199g_1^3g_{1X}g_X + 81g_1g_2^2g_{1X}g_X + 264g_1g_3^2g_{1X}g_X + 199g_1g_{1X}^3g_X + 199g_1^4g_{X1} \right. \\
& + 81g_1^2g_2^2g_{X1} + 264g_1^2g_3^2g_{X1} + 199g_1^2g_{1X}^2g_{X1} + 398g_1^3g_X^2x_H + 162g_1g_2^2g_X^2x_H \\
& + 528g_1g_3^2g_X^2x_H + 1194g_1g_{1X}^2g_X^2x_H + 1990g_1^2g_{1X}g_Xg_{X1}x_H + 162g_2^2g_{1X}g_Xg_{X1}x_H \\
& + 528g_3^2g_{1X}g_Xg_{X1}x_H + 398g_{1X}^3g_Xg_{X1}x_H + 1592g_1^3g_{X1}^2x_H + 324g_1g_2^2g_{X1}^2x_H \\
& + 1056g_1g_3^2g_{X1}^2x_H + 796g_1g_{1X}^2g_{X1}^2x_H + 2388g_1g_{1X}g_X^3x_H^2 + 3184g_1^2g_X^2g_{X1}x_H^2 \\
& + 324g_2^2g_X^2g_{X1}x_H^2 + 1056g_3^2g_X^2g_{X1}x_H^2 + 2388g_{1X}^2g_X^2g_{X1}x_H^2 + 5572g_1g_{1X}g_Xg_{X1}^2x_H^2 \\
& + 4776g_1^2g_{X1}^3x_H^2 + 324g_2^2g_{X1}^3x_H^2 + 1056g_3^2g_{X1}^3x_H^2 + 796g_{1X}^2g_{X1}^3x_H^2 + 1592g_1g_{X1}^4x_H^3 \\
& + 4776g_{1X}g_X^3g_{X1}x_H^3 + 7960g_1g_X^2g_{X1}^2x_H^3 + 4776g_{1X}g_Xg_{X1}^3x_H^3 + 6368g_1g_{X1}^4x_H^3 \\
& + 3184g_{X1}^4g_{X1}^4x_H^4 + 6368g_X^2g_{X1}^3x_H^4 + 3184g_{X1}^5x_H^4 + 82g_1^3g_X^2x_\Phi + 54g_1g_2^2g_X^2x_\Phi + 48g_1g_3^2g_X^2x_\Phi \\
& + 246g_1g_{1X}^2g_X^2x_\Phi + 410g_1^2g_{1X}g_Xg_{X1}x_\Phi + 54g_2^2g_{1X}g_Xg_{X1}x_\Phi + 48g_3^2g_{1X}g_Xg_{X1}x_\Phi \\
& + 82g_{1X}^3g_Xg_{X1}x_\Phi + 328g_1^3g_{X1}^2x_\Phi + 108g_1g_2^2g_{X1}^2x_\Phi + 96g_1g_3^2g_{X1}^2x_\Phi + 164g_1g_{1X}^2g_{X1}^2x_\Phi \\
& + 984g_1g_{1X}g_X^3x_Hx_\Phi + 1312g_1^2g_X^2g_{X1}x_Hx_\Phi + 216g_2^2g_X^2g_{X1}x_Hx_\Phi + 192g_3^2g_X^2g_{X1}x_Hx_\Phi \\
& + 984g_{1X}^2g_X^2g_{X1}x_Hx_\Phi + 2296g_1g_{1X}g_Xg_{X1}^2x_Hx_\Phi + 1968g_1^2g_{X1}^3x_Hx_\Phi + 216g_2^2g_{X1}^3x_Hx_\Phi \\
& + 192g_3^2g_{X1}^3x_Hx_\Phi + 328g_{1X}^2g_{X1}^3x_Hx_\Phi + 984g_1g_X^4x_H^2x_\Phi + 2952g_{1X}g_X^3g_{X1}x_H^2x_\Phi \\
& + 4920g_1g_X^2g_{X1}^2x_H^2x_\Phi + 2952g_{1X}g_Xg_{X1}^3x_H^2x_\Phi + 3936g_{X1}^4x_H^2x_\Phi + 2624g_X^4g_{X1}x_H^3x_\Phi \\
& + 5248g_X^2g_{X1}^3x_H^3x_\Phi + 2624g_{X1}^5x_H^3x_\Phi + 138g_1g_{1X}g_X^3x_\Phi^2 + 184g_1^2g_X^2g_{X1}x_\Phi^2 + 54g_2^2g_X^2g_{X1}x_\Phi^2 \\
& + 48g_3^2g_X^2g_{X1}x_\Phi^2 + 138g_{1X}^2g_X^2g_{X1}x_\Phi^2 + 322g_1g_{1X}g_Xg_{X1}^2x_\Phi^2 + 276g_1^2g_{X1}^3x_\Phi^2 + 54g_2^2g_{X1}^3x_\Phi^2 \\
& + 48g_3^2g_{X1}^3x_\Phi^2 + 46g_{1X}^2g_{X1}^3x_\Phi^2 + 276g_1g_X^4x_Hx_\Phi^2 + 828g_{1X}g_X^3g_{X1}x_Hx_\Phi^2 + 1380g_1g_X^2g_{X1}^2x_Hx_\Phi^2 \\
& + 828g_{1X}g_Xg_{X1}^3x_Hx_\Phi^2 + 1104g_1g_{X1}^4x_Hx_\Phi^2 + 1104g_X^4g_{X1}x_H^2x_\Phi^2 + 2208g_X^2g_{X1}^3x_H^2x_\Phi^2 \\
& + 1104g_{X1}^5x_H^2x_\Phi^2 + 28g_1g_X^4x_\Phi^3 + 84g_{1X}g_X^3g_{X1}x_\Phi^3 + 140g_1g_X^2g_{X1}^2x_\Phi^3 + 84g_{1X}g_Xg_{X1}^3x_\Phi^3 \\
& + 112g_1g_{X1}^4x_\Phi^3 + 224g_X^4g_{X1}x_Hx_\Phi^3 + 448g_X^2g_{X1}^3x_Hx_\Phi^3 + 224g_{X1}^5x_Hx_\Phi^3 + 100g_X^4g_{X1}x_\Phi^4 \\
& + 200g_X^2g_{X1}^3x_\Phi^4 + 100g_{X1}^5x_\Phi^4 - 54g_X^2g_{X1}^2x_\Phi^2y_M^2 - 54g_{X1}^3x_\Phi^2y_M^2 - 51g_1g_{1X}g_Xy_t^2 - 51g_1^2g_{X1}y_t^2 \\
& - 102g_1g_X^2x_Hy_t^2 - 102g_{1X}g_Xg_{X1}x_Hy_t^2 - 204g_1g_{X1}^2x_Hy_t^2 - 204g_X^2g_{X1}x_H^2y_t^2 - 204g_{X1}^3x_H^2y_t^2 \\
& - 15g_1g_X^2x_\Phi y_t^2 - 15g_{1X}g_Xg_{X1}x_\Phi y_t^2 - 30g_1g_{X1}^2x_\Phi y_t^2 - 60g_X^2g_{X1}x_Hx_\Phi y_t^2 - 60g_{X1}^3x_Hx_\Phi y_t^2 \\
& \left. - 6g_X^2g_{X1}x_\Phi^2y_t^2 - 6g_{X1}^3x_\Phi^2y_t^2 \right],
\end{aligned}$$



$$\begin{aligned}
\beta_{g_{1X}}^{(2)} = & \frac{1}{(16\pi^2)^2} \cdot \frac{1}{18} \left[ 199g_1^4g_{1X} + 81g_1^2g_2^2g_{1X} + 264g_1^2g_3^2g_{1X} + 398g_1^2g_{1X}^3 + 81g_2^2g_{1X}^3 \right. \\
& + 264g_3^2g_{1X}^3 + 199g_{1X}^5 + 398g_1^4g_Xx_H + 162g_1^2g_2^2g_Xx_H + 528g_1^2g_3^2g_Xx_H + 1990g_1^2g_{1X}^2g_Xx_H \\
& + 324g_2^2g_{1X}^2g_Xx_H + 1056g_3^2g_{1X}^2g_Xx_H + 1592g_{1X}^4g_Xx_H + 1194g_1^3g_{1X}g_{X1}x_H \\
& + 162g_1g_2^2g_{1X}g_{X1}x_H + 528g_1g_3^2g_{1X}g_{X1}x_H + 1194g_1g_{1X}^3g_{X1}x_H + 3184g_1^2g_{1X}g_X^2x_H^2 \\
& + 324g_2^2g_{1X}g_X^2x_H^2 + 1056g_3^2g_{1X}g_X^2x_H^2 + 4776g_{1X}^3g_X^2x_H^2 + 2388g_1^3g_Xg_{X1}x_H^2 \\
& + 324g_1g_2^2g_Xg_{X1}x_H^2 + 1056g_1g_3^2g_Xg_{X1}x_H^2 + 5572g_1g_{1X}^2g_Xg_{X1}x_H^2 + 2388g_1^2g_{1X}g_{X1}^2x_H^2 \\
& + 796g_{1X}^3g_{X1}^2x_H^2 + 1592g_1^3g_X^3x_H^3 + 6368g_{1X}^2g_X^3x_H^3 + 7960g_1g_{1X}g_X^2g_{X1}x_H^3 + 4776g_1^2g_Xg_{X1}^2x_H^3 \\
& + 3184g_{1X}^2g_Xg_{X1}^2x_H^3 + 1592g_1g_{1X}g_{X1}^3x_H^3 + 3184g_{1X}g_X^4x_H^4 + 3184g_1g_X^3g_{X1}x_H^4 \\
& + 3184g_{1X}g_X^2g_{X1}^2x_H^4 + 3184g_1g_Xg_{X1}^3x_H^4 + 82g_1^4g_Xx_\Phi + 54g_1^2g_2^2g_Xx_\Phi + 48g_1^2g_3^2g_Xx_\Phi \\
& + 410g_1^2g_{1X}^2g_Xx_\Phi + 108g_2^2g_{1X}^2g_Xx_\Phi + 96g_3^2g_{1X}^2g_Xx_\Phi + 328g_{1X}^4g_Xx_\Phi + 246g_1^3g_{1X}g_{X1}x_\Phi \\
& + 54g_1g_2^2g_{1X}g_{X1}x_\Phi + 48g_1g_3^2g_{1X}g_{X1}x_\Phi + 246g_1g_{1X}^3g_{X1}x_\Phi + 1312g_1^2g_{1X}g_X^2x_Hx_\Phi \\
& + 216g_2^2g_{1X}g_X^2x_Hx_\Phi + 192g_3^2g_{1X}g_X^2x_Hx_\Phi + 1968g_{1X}^3g_X^2x_Hx_\Phi + 984g_1^3g_Xg_{X1}x_Hx_\Phi \\
& + 216g_1g_2^2g_Xg_{X1}x_Hx_\Phi + 192g_1g_3^2g_Xg_{X1}x_Hx_\Phi + 2296g_1g_{1X}^2g_Xg_{X1}x_Hx_\Phi + 984g_1^2g_{1X}g_{X1}^2x_Hx_\Phi \\
& + 328g_{1X}^3g_{X1}^2x_Hx_\Phi + 984g_1^2g_X^3x_H^2x_\Phi + 3936g_{1X}^2g_X^3x_H^2x_\Phi + 4920g_1g_{1X}g_X^2g_{X1}x_H^2x_\Phi \\
& + 2952g_1^2g_Xg_{X1}^2x_H^2x_\Phi + 1968g_{1X}^2g_Xg_{X1}^2x_H^2x_\Phi + 984g_1g_{1X}g_{X1}^3x_H^2x_\Phi + 2624g_{1X}g_X^4x_H^3x_\Phi \\
& + 2624g_1g_X^3g_{X1}x_H^3x_\Phi + 2624g_{1X}g_X^2g_{X1}^2x_H^3x_\Phi + 2624g_1g_Xg_{X1}^3x_H^3x_\Phi + 184g_1^2g_{1X}g_X^2x_\Phi^2 \\
& + 54g_2^2g_{1X}g_X^2x_\Phi^2 + 48g_3^2g_{1X}g_X^2x_\Phi^2 + 276g_{1X}^3g_X^2x_\Phi^2 + 138g_1^3g_Xg_{X1}x_\Phi^2 + 54g_1g_2^2g_Xg_{X1}x_\Phi^2 \\
& + 48g_1g_3^2g_Xg_{X1}x_\Phi^2 + 322g_1g_{1X}^2g_Xg_{X1}x_\Phi^2 + 138g_1^2g_{1X}g_{X1}^2x_\Phi^2 + 46g_{1X}^3g_{X1}^2x_\Phi^2 \\
& + 276g_1^2g_X^3x_Hx_\Phi^2 + 1104g_{1X}^2g_X^3x_Hx_\Phi^2 + 1380g_1g_{1X}g_X^2g_{X1}x_Hx_\Phi^2 + 828g_1^2g_Xg_{X1}^2x_Hx_\Phi^2 \\
& + 552g_{1X}^2g_Xg_{X1}^2x_Hx_\Phi^2 + 276g_1g_{1X}g_{X1}^3x_Hx_\Phi^2 + 1104g_{1X}g_X^4x_H^2x_\Phi^2 + 1104g_1g_X^3g_{X1}x_H^2x_\Phi^2 \\
& + 1104g_{1X}g_X^2g_{X1}^2x_H^2x_\Phi^2 + 1104g_1g_Xg_{X1}^3x_H^2x_\Phi^2 + 28g_1^2g_X^3x_\Phi^3 + 112g_{1X}^2g_X^3x_\Phi^3 \\
& + 140g_1g_{1X}g_X^2g_{X1}x_\Phi^3 + 84g_1^2g_Xg_{X1}^2x_\Phi^3 + 56g_{1X}^2g_Xg_{X1}^2x_\Phi^3 + 28g_1g_{1X}g_{X1}^3x_\Phi^3 \\
& + 224g_{1X}g_X^4x_Hx_\Phi^3 + 224g_1g_X^3g_{X1}x_Hx_\Phi^3 + 224g_{1X}g_X^2g_{X1}^2x_Hx_\Phi^3 + 224g_1g_Xg_{X1}^3x_Hx_\Phi^3 \\
& + 100g_{1X}g_X^4x_\Phi^4 + 100g_1g_X^3g_{X1}x_\Phi^4 + 100g_{1X}g_X^2g_{X1}^2x_\Phi^4 + 100g_1g_Xg_{X1}^3x_\Phi^4 - 54g_{1X}g_X^2x_\Phi^2y_M^2 \\
& - 54g_1g_Xg_{X1}x_\Phi^2y_M^2 - 51g_1^2g_{1X}y_t^2 - 51g_{1X}^3y_t^2 - 102g_1^2g_Xx_Hy_t^2 - 204g_{1X}^2g_Xx_Hy_t^2 \\
& - 102g_1g_{1X}g_{X1}x_Hy_t^2 - 204g_{1X}g_X^2x_Hy_t^2 - 204g_1g_Xg_{X1}x_Hy_t^2 - 15g_1^2g_Xx_\Phi y_t^2 \\
& - 30g_{1X}^2g_Xx_\Phi y_t^2 - 15g_1g_{1X}g_{X1}x_\Phi y_t^2 - 60g_{1X}g_X^2x_Hx_\Phi y_t^2 - 60g_1g_Xg_{X1}x_Hx_\Phi y_t^2 \\
& \left. - 6g_{1X}g_X^2x_\Phi^2y_t^2 - 6g_1g_Xg_{X1}x_\Phi^2y_t^2 \right],
\end{aligned}$$

$$\begin{aligned}
\beta_{g_X}^{(2)} = & \frac{1}{(16\pi^2)^2} \cdot \frac{1}{18} \left[ 199g_1^2g_{1X}^2g_X + 81g_2^2g_{1X}^2g_X + 264g_3^2g_{1X}^2g_X + 199g_{1X}^4g_X + 199g_1^3g_{1X}g_{X1} \right. \\
& + 81g_1g_2^2g_{1X}g_{X1} + 264g_1g_3^2g_{1X}g_{X1} + 199g_1g_{1X}^3g_{X1} + 796g_1^2g_{1X}g_X^2x_H \\
& + 324g_2^2g_{1X}g_X^2x_H + 1056g_3^2g_{1X}g_X^2x_H + 1592g_{1X}^3g_X^2x_H + 398g_1^3g_Xg_{X1}x_H \\
& + 162g_1g_2^2g_Xg_{X1}x_H + 528g_1g_3^2g_Xg_{X1}x_H + 1990g_1g_{1X}^2g_Xg_{X1}x_H + 1194g_1^2g_{1X}g_X^2x_H \\
& + 162g_2^2g_{1X}g_X^2x_H + 528g_3^2g_{1X}g_X^2x_H + 398g_{1X}^3g_X^2x_H + 796g_1^2g_X^3x_H^2 + 324g_2^2g_X^3x_H^2 \\
& + 1056g_3^2g_X^3x_H^2 + 4776g_{1X}^2g_X^3x_H^2 + 5572g_1g_{1X}g_X^2g_{X1}x_H^2 + 2388g_1^2g_Xg_X^2x_H^2 \\
& + 324g_2^2g_Xg_X^2x_H^2 + 1056g_3^2g_Xg_X^2x_H^2 + 3184g_{1X}^2g_Xg_X^2x_H^2 + 2388g_1g_{1X}g_X^3x_H^2 \\
& + 6368g_{1X}g_X^4x_H^3 + 4776g_1g_X^3g_{X1}x_H^3 + 7960g_{1X}g_X^2g_X^2x_H^3 + 4776g_1g_Xg_X^3x_H^3 \\
& + 1592g_{1X}g_X^4x_H^3 + 3184g_X^5x_H^4 + 6368g_X^3g_X^2x_H^4 + 3184g_Xg_X^4x_H^4 + 164g_1^2g_{1X}g_X^2x_\Phi \\
& + 108g_2^2g_{1X}g_X^2x_\Phi + 96g_3^2g_{1X}g_X^2x_\Phi + 328g_{1X}^3g_X^2x_\Phi + 82g_1^3g_Xg_{X1}x_\Phi + 54g_1g_2^2g_Xg_{X1}x_\Phi \\
& + 48g_1g_3^2g_Xg_{X1}x_\Phi + 410g_1g_{1X}^2g_Xg_{X1}x_\Phi + 246g_1^2g_{1X}g_X^2x_\Phi + 54g_2^2g_{1X}g_X^2x_\Phi \\
& + 48g_3^2g_{1X}g_X^2x_\Phi + 82g_{1X}^3g_X^2x_\Phi + 328g_1^2g_X^3x_Hx_\Phi + 216g_2^2g_X^3x_Hx_\Phi + 192g_3^2g_X^3x_Hx_\Phi \\
& + 1968g_{1X}^2g_X^3x_Hx_\Phi + 2296g_1g_{1X}g_X^2g_{X1}x_Hx_\Phi + 984g_1^2g_Xg_X^2x_Hx_\Phi + 216g_2^2g_Xg_X^2x_Hx_\Phi \\
& + 192g_3^2g_Xg_X^2x_Hx_\Phi + 1312g_{1X}^2g_Xg_X^2x_Hx_\Phi + 984g_1g_{1X}g_X^3x_Hx_\Phi + 3936g_{1X}g_X^4x_H^2x_\Phi \\
& + 2952g_1g_X^3g_{X1}x_H^2x_\Phi + 4920g_{1X}g_X^2g_X^2x_H^2x_\Phi + 2952g_1g_Xg_X^3x_H^2x_\Phi + 984g_{1X}g_X^4x_H^2x_\Phi \\
& + 2624g_X^5x_H^3x_\Phi + 5248g_X^3g_X^2x_H^3x_\Phi + 2624g_Xg_X^4x_H^3x_\Phi + 46g_1^2g_X^3x_\Phi^2 + 54g_2^2g_X^3x_\Phi^2 \\
& + 48g_3^2g_X^3x_\Phi^2 + 276g_{1X}^2g_X^3x_\Phi^2 + 322g_1g_{1X}g_X^2g_{X1}x_\Phi^2 + 138g_1^2g_Xg_X^2x_\Phi^2 + 54g_2^2g_Xg_X^2x_\Phi^2 \\
& + 48g_3^2g_Xg_X^2x_\Phi^2 + 184g_{1X}^2g_Xg_X^2x_\Phi^2 + 138g_1g_{1X}g_X^3x_\Phi^2 + 1104g_{1X}g_X^4x_Hx_\Phi^2 \\
& + 828g_1g_X^3g_{X1}x_Hx_\Phi^2 + 1380g_{1X}g_X^2g_X^2x_Hx_\Phi^2 + 828g_1g_Xg_X^3x_Hx_\Phi^2 + 276g_{1X}g_X^4x_Hx_\Phi^2 \\
& + 1104g_X^5x_H^2x_\Phi^2 + 2208g_X^3g_X^2x_H^2x_\Phi^2 + 1104g_Xg_X^4x_H^2x_\Phi^2 + 112g_{1X}g_X^4x_\Phi^3 + 84g_1g_X^3g_{X1}x_\Phi^3 \\
& + 140g_{1X}g_X^2g_X^2x_\Phi^3 + 84g_1g_Xg_X^3x_\Phi^3 + 28g_{1X}g_X^4x_\Phi^3 + 224g_X^5x_Hx_\Phi^3 + 448g_X^3g_X^2x_Hx_\Phi^3 \\
& + 224g_Xg_X^4x_Hx_\Phi^3 + 100g_X^5x_\Phi^4 + 200g_X^3g_X^2x_\Phi^4 + 100g_Xg_X^4x_\Phi^4 - 54g_X^3x_\Phi^2y_M^2 - 54g_Xg_X^2x_\Phi^2y_M^2 \\
& - 51g_{1X}^2g_Xy_t^2 - 51g_1g_{1X}g_{X1}y_t^2 - 204g_{1X}g_X^2x_Hy_t^2 - 102g_1g_Xg_{X1}x_Hy_t^2 - 102g_{1X}g_X^2x_Hy_t^2 \\
& - 204g_X^3x_Hy_t^2 - 204g_Xg_X^2x_H^2y_t^2 - 30g_{1X}g_X^2x_\Phi y_t^2 - 15g_1g_Xg_{X1}x_\Phi y_t^2 - 15g_{1X}g_X^2x_\Phi y_t^2 \\
& \left. - 60g_X^3x_Hx_\Phi y_t^2 - 60g_Xg_X^2x_Hx_\Phi y_t^2 - 6g_X^3x_\Phi^2y_t^2 - 6g_Xg_X^2x_\Phi^2y_t^2 \right]. \tag{A.3}
\end{aligned}$$

## A.2 The U(1)' RGEs for the Yukawa couplings

The RGEs for the Yukawa couplings at the two-loop level are given by

$$\mu \frac{dy_i}{d\mu} = \beta_{y_i}^{(1)} + \beta_{y_i}^{(2)}, \tag{A.4}$$

where  $\beta_{y_i}^{(1)}$  and  $\beta_{y_i}^{(2)}$  are the one-loop and two-loop beta functions for the Yukawa couplings, respectively, and  $y_i$  represents  $y_t$  and  $y_M$ . Here, the one-loop beta functions for the Yukawa

couplings are given by

$$\begin{aligned}
\beta_{y_t}^{(1)} &= \frac{y_t}{16\pi^2} \left[ \frac{9}{2}y_t^2 - 8g_3^2 - \frac{9}{4}g_2^2 - \frac{1}{6}(g_1 + 2x_H g_{X1} + x_\Phi g_{X1})(4g_1 + 8x_H g_{X1} + x_\Phi g_{X1}) \right. \\
&\quad - \frac{3}{4}(g_1 + 2x_H g_{X1})^2 - \frac{1}{6}(g_{1X} + 2x_H g_X + x_\Phi g_X)(4g_{1X} + 8x_H g_X + x_\Phi g_X) \\
&\quad \left. - \frac{3}{4}(g_{1X} + 2x_H g_X)^2 \right], \\
\beta_{y_M}^{(1)} &= \frac{y_M}{16\pi^2} \left[ 10y_M^2 - \frac{3}{2}x_\Phi^2 (g_{X1}^2 + g_X^2) \right], \tag{A.5}
\end{aligned}$$

and the two-loop beta functions for the Yukawa couplings are given by

$$\begin{aligned}
\beta_{y_t}^{(2)} &= \frac{1}{(16\pi^2)^2} \cdot \frac{1}{432} \left[ -9(-72y_t^5 - y_t^3(223g_1^2 + 405g_2^2 + 768g_3^2 + 223g_{1X}^2 + 892g_{1X}g_Xx_H \right. \\
&\quad + 892g_1g_{X1}x_H + 892g_X^2x_H^2 + 892g_{X1}^2x_H^2 + 50g_{1X}g_Xx_\Phi + 50g_1g_{X1}x_\Phi + 100g_X^2x_Hx_\Phi \\
&\quad + 100g_{X1}^2x_Hx_\Phi + 16g_X^2x_\Phi^2 + 16g_{X1}^2x_\Phi^2 - 324y_t^2 - 576\lambda_H)) \\
&\quad + y_t(2374g_1^4 - 324g_1^2g_2^2 - 2484g_2^4 + 912g_1^2g_3^2 + 3888g_2^2g_3^2 - 46656g_3^4 + 4748g_1^2g_{1X}^2 \\
&\quad - 324g_2^2g_{1X}^2 + 912g_3^2g_{1X}^2 + 2374g_{1X}^4 + 18992g_{1X}^2g_Xx_H - 1296g_2^2g_{1X}g_Xx_H \\
&\quad + 3648g_3^2g_{1X}g_Xx_H + 18992g_{1X}^3g_Xx_H + 18992g_1^3g_{X1}x_H - 1296g_1g_2^2g_{X1}x_H \\
&\quad + 3648g_1g_3^2g_{X1}x_H + 18992g_1g_{1X}^2g_{X1}x_H + 18992g_1^2g_X^2x_H^2 - 1296g_2^2g_X^2x_H^2 \\
&\quad + 3648g_3^2g_X^2x_H^2 + 56976g_{1X}^2g_X^2x_H^2 + 75968g_1g_{1X}g_Xg_{X1}x_H^2 + 56976g_2^2g_{X1}^2x_H^2 \\
&\quad - 1296g_2^2g_{X1}^2x_H^2 + 3648g_3^2g_{X1}^2x_H^2 + 18992g_{1X}^2g_{X1}^2x_H^2 + 75968g_{1X}g_X^3x_H^3 \\
&\quad + 75968g_1g_X^2g_{X1}x_H^3 + 75968g_{1X}g_Xg_{X1}^3x_H^3 + 75968g_1g_{X1}^3x_H^3 + 37984g_X^4x_H^4 \\
&\quad + 75968g_X^2g_{X1}^2x_H^4 + 37984g_{X1}^4x_H^4 + 4016g_1^2g_{1X}g_Xx_\Phi + 486g_2^2g_{1X}g_Xx_\Phi \\
&\quad - 480g_3^2g_{1X}g_Xx_\Phi + 4016g_{1X}^3g_Xx_\Phi + 4016g_1^3g_{X1}x_\Phi + 486g_1g_2^2g_{X1}x_\Phi - 480g_1g_3^2g_{X1}x_\Phi \\
&\quad + 4016g_1g_{1X}^2g_{X1}x_\Phi + 8032g_1^2g_X^2x_Hx_\Phi + 972g_2^2g_X^2x_Hx_\Phi - 960g_3^2g_X^2x_Hx_\Phi \\
&\quad + 24096g_{1X}^2g_X^2x_Hx_\Phi + 32128g_1g_{1X}g_Xg_{X1}x_Hx_\Phi + 24096g_1^2g_{X1}^2x_Hx_\Phi + 972g_2^2g_{X1}^2x_Hx_\Phi \\
&\quad - 960g_3^2g_{X1}^2x_Hx_\Phi + 8032g_{1X}^2g_{X1}^2x_Hx_\Phi + 48192g_{1X}g_X^3x_H^2x_\Phi + 48192g_1g_X^2g_{X1}x_H^2x_\Phi \\
&\quad + 48192g_{1X}g_Xg_{X1}^2x_H^2x_\Phi + 48192g_1g_{X1}^3x_H^2x_\Phi + 32128g_X^4x_H^3x_\Phi + 64256g_X^2g_{X1}^2x_H^3x_\Phi \\
&\quad + 32128g_{X1}^4x_H^3x_\Phi + 819g_1^2g_X^2x_\Phi^2 + 81g_2^2g_X^2x_\Phi^2 - 96g_3^2g_X^2x_\Phi^2 + 3255g_{1X}^2g_X^2x_\Phi^2 \\
&\quad + 4872g_1g_{1X}g_Xg_{X1}x_\Phi^2 + 3255g_1^2g_{X1}^2x_\Phi^2 + 81g_2^2g_{X1}^2x_\Phi^2 - 96g_3^2g_{X1}^2x_\Phi^2 + 819g_{1X}^2g_{X1}^2x_\Phi^2 \\
&\quad + 13020g_{1X}g_X^3x_Hx_\Phi^2 + 13020g_1g_X^2g_{X1}x_Hx_\Phi^2 + 13020g_{1X}g_Xg_{X1}^2x_Hx_\Phi^2 + 13020g_1g_{X1}^3x_Hx_\Phi^2 \\
&\quad + 13020g_X^4x_H^2x_\Phi^2 + 26040g_X^2g_{X1}^2x_H^2x_\Phi^2 + 13020g_{X1}^4x_H^2x_\Phi^2 + 1330g_{1X}g_X^3x_\Phi^3 \\
&\quad + 1330g_1g_X^2g_{X1}x_\Phi^3 + 1330g_{1X}g_Xg_{X1}^2x_\Phi^3 + 1330g_1g_{X1}^3x_\Phi^3 + 2660g_X^4x_Hx_\Phi^3 + 5320g_X^2g_{X1}^2x_Hx_\Phi^3 \\
&\quad + 2660g_{X1}^4x_Hx_\Phi^3 + 203g_X^4x_\Phi^4 + 406g_X^2g_{X1}^2x_\Phi^4 + 203g_{X1}^4x_\Phi^4 + 1530g_1^2y_t^2 + 2430g_2^2y_t^2 \\
&\quad + 8640g_3^2y_t^2 + 1530g_{1X}^2y_t^2 + 6120g_{1X}g_Xx_Hy_t^2 + 6120g_1g_{X1}x_Hy_t^2 + 6120g_X^2x_Hy_t^2 \\
&\quad + 6120g_{X1}^2x_Hy_t^2 + 900g_{1X}g_Xx_\Phi y_t^2 + 900g_1g_{X1}x_\Phi y_t^2 + 1800g_X^2x_Hx_\Phi y_t^2 + 1800g_{X1}^2x_Hx_\Phi y_t^2 \\
&\quad \left. + 180g_X^2x_\Phi^2y_t^2 + 180g_{X1}^2x_\Phi^2y_t^2 - 2916y_t^4 + 2592\lambda_H^2 + 216\lambda_{\text{mix}}^2) \right],
\end{aligned}$$

$$\begin{aligned}
\beta_{y_M}^{(2)} = & \frac{1}{(16\pi^2)^2} \cdot \frac{1}{48} \left[ y_M \left( -70g_{1X}^2 g_X^2 x_\Phi^2 - 140g_1 g_{1X} g_X g_{X1} x_\Phi^2 - 70g_1^2 g_{X1}^2 x_\Phi^2 - 280g_{1X} g_X^3 x_H x_\Phi^2 \right. \right. \\
& - 280g_1 g_X^2 g_{X1} x_H x_\Phi^2 - 280g_{1X} g_X g_{X1}^2 x_H x_\Phi^2 - 280g_1 g_{X1}^3 x_H x_\Phi^2 - 280g_X^4 x_H^2 x_\Phi^2 \\
& - 560g_X^2 g_{X1}^2 x_H^2 x_\Phi^2 - 280g_{X1}^4 x_H^2 x_\Phi^2 - 64g_{1X} g_X^3 x_\Phi^3 - 64g_1 g_X^2 g_{X1} x_\Phi^3 - 64g_{1X} g_X g_{X1}^2 x_\Phi^3 \\
& - 64g_1 g_{X1}^3 x_\Phi^3 - 128g_X^4 x_H x_\Phi^3 - 256g_X^2 g_{X1}^2 x_H x_\Phi^3 - 128g_{X1}^4 x_H x_\Phi^3 - 381g_X^4 x_\Phi^4 - 762g_X^2 g_{X1}^2 x_\Phi^4 \\
& - 381g_{X1}^4 x_\Phi^4 + 360(g_X^2 + g_{X1}^2) x_\Phi^2 y_M^2 - 1728y_M^4 + 48\lambda_{\text{mix}}^2 + 192\lambda_\Phi^2 \Big) \\
& + 6(224y_M^5 - 32y_M^3(-11(g_X^2 + g_{X1}^2)x_\Phi^2 + 9y_M^2 + 8\lambda_\Phi)) \Big]. \tag{A.6}
\end{aligned}$$

### A.3 The U(1)' RGEs for the scalar quartic couplings

Finally, the RGEs for the scalar quartic couplings at the two-loop level are given by

$$\mu \frac{d\lambda_i}{d\mu} = \beta_{\lambda_i}^{(1)} + \beta_{\lambda_i}^{(2)}, \tag{A.7}$$

where  $\beta_{\lambda_i}^{(1)}$  and  $\beta_{\lambda_i}^{(2)}$  are the one-loop and two-loop beta functions for the scalar quartic couplings, respectively, and  $\lambda_i$  represents  $\lambda_H$ ,  $\lambda_\Phi$  and  $\lambda_{\text{mix}}$ . Here, the one-loop beta functions for the scalar quartic couplings are given by

$$\begin{aligned}
\beta_{\lambda_H}^{(1)} = & \frac{1}{16\pi^2} \left[ \lambda_H \left\{ 24\lambda_H + 12y_t^2 - 9g_2^2 - 3(g_1 + 2x_H g_{X1})^2 - 3(g_{1X} + 2x_H g_X)^2 \right\} \right. \\
& + \lambda_{\text{mix}}^2 - 6y_t^4 + \frac{9}{8}g_2^4 + \frac{3}{8} \left\{ (g_1 + 2x_H g_{X1})^2 + (g_{1X} + 2x_H g_X)^2 \right\}^2 \\
& + \frac{3}{4}g_2^2(g_1 + 2x_H g_{X1})^2 + \frac{3}{4}g_2^2(g_{1X} + 2x_H g_X)^2 \Big], \\
\beta_{\lambda_\Phi}^{(1)} = & \frac{1}{16\pi^2} \left[ \lambda_\Phi \left\{ 20\lambda_\Phi + 24y_M^2 - 12(x_\Phi g_{X1})^2 - 12(x_\Phi g_X)^2 \right\} \right. \\
& + 2\lambda_{\text{mix}}^2 - 48y_M^4 + 6 \left\{ (x_\Phi g_{X1})^2 + (x_\Phi g_X)^2 \right\}^2 \Big], \\
\beta_{\lambda_{\text{mix}}}^{(1)} = & \frac{1}{16\pi^2} \left[ \lambda_{\text{mix}} \left\{ 12\lambda_H + 8\lambda_\Phi + 4\lambda_{\text{mix}} + 6y_t^2 + 12y_M^2 \right. \right. \\
& - \frac{9}{2}g_2^2 - \frac{3}{2}(g_1 + 2x_H g_{X1})^2 - 6(x_\Phi g_{X1})^2 - \frac{3}{2}(g_{1X} + 2x_H g_X)^2 - 6(x_\Phi g_X)^2 \Big\} \\
& + 3 \left\{ (g_1 + 2x_H g_{X1})(x_\Phi g_{X1}) + (g_{1X} + 2x_H g_X)(x_\Phi g_X) \right\}^2 \Big], \tag{A.8}
\end{aligned}$$

and the two-loop beta functions for the scalar quartic couplings are given by

$$\begin{aligned}
\beta_{\lambda_H}^{(2)} = & \frac{1}{(16\pi^2)^2} \left[ -\frac{379g_1^6}{48} - \frac{559}{48}g_1^4g_2^2 - \frac{289}{48}g_1^2g_2^4 + \frac{305g_2^6}{16} - \frac{469}{48}g_1^4g_{1X}^2 - \frac{75}{8}g_1^2g_2^2g_{1X}^2 \right. \\
& - \frac{289}{48}g_2^4g_{1X}^2 - \frac{469}{48}g_1^2g_{1X}^4 - \frac{559}{48}g_2^2g_{1X}^4 - \frac{379g_{1X}^6}{48} - \frac{469}{12}g_1^4g_{1X}g_Xx_H \\
& - \frac{75}{2}g_1^2g_2^2g_{1X}g_Xx_H - \frac{289}{12}g_2^4g_{1X}g_Xx_H - \frac{469}{6}g_1^2g_{1X}^3g_Xx_H - \frac{559}{6}g_2^2g_{1X}^3g_Xx_H \\
& - \frac{379}{4}g_{1X}^5g_Xx_H - \frac{379}{4}g_1^5g_{X1}x_H - \frac{559}{6}g_1^3g_2^2g_{X1}x_H - \frac{289}{12}g_1g_2^4g_{X1}x_H - \frac{469}{6}g_1^3g_{1X}^2g_{X1}x_H \\
& - \frac{75}{2}g_1g_2^2g_{1X}^2g_{X1}x_H - \frac{469}{12}g_1g_{1X}^4g_{X1}x_H - \frac{469}{12}g_1^4g_X^2x_H^2 - \frac{75}{2}g_1^2g_2^2g_X^2x_H^2 - \frac{289}{12}g_2^4g_X^2x_H^2 \\
& - \frac{469}{2}g_1^2g_{1X}^2g_X^2x_H^2 - \frac{559}{2}g_2^2g_{1X}^2g_X^2x_H^2 - \frac{1895}{4}g_{1X}^4g_X^2x_H^2 - \frac{938}{3}g_1^3g_{1X}g_Xg_{X1}x_H^2 \\
& - 150g_1g_2^2g_{1X}g_Xg_{X1}x_H^2 - \frac{938}{3}g_1g_{1X}^3g_Xg_{X1}x_H^2 - \frac{1895}{4}g_1^4g_{X1}^2x_H^2 - \frac{559}{2}g_1^2g_2^2g_{X1}^2x_H^2 \\
& - \frac{289}{12}g_2^4g_{X1}^2x_H^2 - \frac{469}{2}g_1^2g_{1X}^2g_{X1}^2x_H^2 - \frac{75}{2}g_2^2g_{1X}^2g_{X1}^2x_H^2 - \frac{469}{12}g_{1X}^4g_{X1}^2x_H^2 - \frac{938}{3}g_1^2g_{1X}g_X^3x_H^3 \\
& - \frac{1118}{3}g_2^2g_{1X}g_X^3x_H^3 - \frac{3790}{3}g_{1X}^3g_X^3x_H^3 - \frac{938}{3}g_1^3g_X^2g_{X1}x_H^3 - 150g_1g_2^2g_X^2g_{X1}x_H^3 \\
& - 938g_1g_{1X}^2g_X^2g_{X1}x_H^3 - 938g_1^2g_{1X}g_Xg_{X1}^2x_H^3 - 150g_2^2g_{1X}g_Xg_{X1}^2x_H^3 - \frac{938}{3}g_{1X}^3g_Xg_{X1}^2x_H^3 \\
& - \frac{3790}{3}g_1^3g_{X1}^3x_H^3 - \frac{1118}{3}g_1g_2^2g_{X1}^3x_H^3 - \frac{938}{3}g_1g_{1X}^2g_{X1}^3x_H^3 - \frac{469}{3}g_1^2g_X^4x_H^4 - \frac{559}{3}g_2^2g_X^4x_H^4 \\
& - 1895g_{1X}^2g_X^4x_H^4 - \frac{3752}{3}g_1g_{1X}g_X^3g_{X1}x_H^4 - 938g_1^2g_X^2g_{X1}^2x_H^4 - 150g_2^2g_X^2g_{X1}^2x_H^4 \\
& - 938g_{1X}^2g_X^2g_{X1}^2x_H^4 - \frac{3752}{3}g_1g_{1X}g_Xg_{X1}^3x_H^4 - 1895g_1^2g_{X1}^4x_H^4 - \frac{559}{3}g_2^2g_{X1}^4x_H^4 \\
& - \frac{469}{3}g_{1X}^2g_{X1}^4x_H^4 - 1516g_{1X}g_X^5x_H^5 - \frac{1876}{3}g_1g_X^4g_{X1}x_H^5 - \frac{3752}{3}g_{1X}g_X^3g_{X1}^2x_H^5 \\
& - \frac{3752}{3}g_1g_X^2g_{X1}^3x_H^5 - \frac{1876}{3}g_{1X}g_Xg_{X1}^4x_H^5 - 1516g_1g_{X1}^5x_H^5 - \frac{1516}{3}g_X^6x_H^6 - \frac{1876}{3}g_X^4g_{X1}^2x_H^6 \\
& - \frac{1876}{3}g_X^2g_{X1}^4x_H^6 - \frac{1516}{3}g_{X1}^6x_H^6 - \frac{16}{3}g_1^2g_{1X}^3g_Xx_\Phi - \frac{16}{3}g_2^2g_{1X}^3g_Xx_\Phi - \frac{16}{3}g_{1X}^5g_Xx_\Phi \\
& - \frac{16}{3}g_1^5g_{X1}x_\Phi - \frac{16}{3}g_1^3g_2^2g_{X1}x_\Phi - \frac{16}{3}g_1^3g_{1X}^2g_{X1}x_\Phi - 32g_1^2g_{1X}^2g_X^2x_Hx_\Phi - 32g_2^2g_{1X}^2g_X^2x_Hx_\Phi \\
& - \frac{160}{3}g_{1X}^4g_X^2x_Hx_\Phi - \frac{64}{3}g_1^3g_{1X}g_Xg_{X1}x_Hx_\Phi - \frac{64}{3}g_1g_{1X}^3g_Xg_{X1}x_Hx_\Phi - \frac{160}{3}g_1^4g_{X1}^2x_Hx_\Phi \\
& - 32g_1^2g_2^2g_{X1}^2x_Hx_\Phi - 32g_1^2g_{1X}^2g_{X1}^2x_Hx_\Phi - 64g_1^2g_{1X}g_X^3x_H^2x_\Phi - 64g_2^2g_{1X}g_X^3x_H^2x_\Phi \\
& - \frac{640}{3}g_{1X}^3g_X^3x_H^2x_\Phi - \frac{64}{3}g_1^3g_X^2g_{X1}x_H^2x_\Phi - 128g_1g_{1X}^2g_X^2g_{X1}x_H^2x_\Phi - 128g_1^2g_{1X}g_Xg_{X1}^2x_H^2x_\Phi \\
& - \frac{64}{3}g_{1X}^3g_Xg_{X1}^2x_H^2x_\Phi - \frac{640}{3}g_1^3g_{X1}^3x_H^2x_\Phi - 64g_1g_2^2g_{X1}^3x_H^2x_\Phi - 64g_1g_{1X}^2g_{X1}^3x_H^2x_\Phi \\
& - \frac{128}{3}g_1^2g_X^4x_H^3x_\Phi - \frac{128}{3}g_2^2g_X^4x_H^3x_\Phi - \frac{1280}{3}g_{1X}^2g_X^4x_H^3x_\Phi - 256g_1g_{1X}g_X^3g_{X1}x_H^3x_\Phi
\end{aligned}$$

$$\begin{aligned}
& - 128g_1^2g_X^2g_{X1}^2x_H^3x_\Phi - 128g_1^2g_X^2g_{X1}^2x_H^3x_\Phi - 256g_1g_1Xg_Xg_{X1}^3x_H^3x_\Phi - \frac{1280}{3}g_1^2g_{X1}^4x_H^3x_\Phi \\
& - \frac{128}{3}g_2^2g_{X1}^4x_H^3x_\Phi - \frac{128}{3}g_1^2g_{X1}^4x_H^3x_\Phi - \frac{1280}{3}g_1Xg_X^5x_H^4x_\Phi - \frac{512}{3}g_1g_X^4g_{X1}^4x_H^4x_\Phi \\
& - 256g_1Xg_X^3g_{X1}^2x_H^4x_\Phi - 256g_1g_X^2g_{X1}^3x_H^4x_\Phi - \frac{512}{3}g_1Xg_Xg_{X1}^4x_H^4x_\Phi - \frac{1280}{3}g_1g_{X1}^5x_H^4x_\Phi \\
& - \frac{512}{3}g_X^6x_H^5x_\Phi - \frac{512}{3}g_X^4g_{X1}^2x_H^5x_\Phi - \frac{512}{3}g_X^2g_{X1}^4x_H^5x_\Phi - \frac{512}{3}g_{X1}^6x_H^5x_\Phi - \frac{13}{4}g_1^2g_{1X}^2g_X^2x_\Phi^2 \\
& - \frac{13}{4}g_2^2g_{1X}^2g_X^2x_\Phi^2 - \frac{13}{4}g_1^4g_X^2x_\Phi^2 - \frac{13}{4}g_1^4g_{X1}^2x_\Phi^2 - \frac{13}{4}g_1^2g_2^2g_{X1}^2x_\Phi^2 - \frac{13}{4}g_1^2g_{1X}^2g_{X1}^2x_\Phi^2 \\
& - 13g_1^2g_1Xg_X^3x_Hx_\Phi^2 - 13g_2^2g_1Xg_X^3x_Hx_\Phi^2 - 26g_1^3g_X^3x_Hx_\Phi^2 - 13g_1g_1^2g_X^2g_{X1}x_Hx_\Phi^2 \\
& - 13g_1^2g_1Xg_Xg_{X1}^2x_Hx_\Phi^2 - 26g_1^3g_{X1}^3x_Hx_\Phi^2 - 13g_1g_2^2g_{X1}^3x_Hx_\Phi^2 - 13g_1g_1^2g_{X1}^3x_Hx_\Phi^2 \\
& - 13g_1^2g_X^4x_H^2x_\Phi^2 - 13g_2^2g_X^4x_H^2x_\Phi^2 - 78g_1^2g_X^4x_H^2x_\Phi^2 - 52g_1g_1Xg_X^3g_{X1}x_H^2x_\Phi^2 - 13g_1^2g_X^2g_{X1}^2x_H^2x_\Phi^2 \\
& - 13g_1^2g_X^2g_{X1}^2x_H^2x_\Phi^2 - 52g_1g_1Xg_Xg_{X1}^2x_H^2x_\Phi^2 - 78g_1^2g_{X1}^4x_H^2x_\Phi^2 - 13g_2^2g_{X1}^4x_H^2x_\Phi^2 \\
& - 13g_1^2g_{X1}^4x_H^2x_\Phi^2 - 104g_1Xg_X^5x_H^3x_\Phi^2 - 52g_1g_X^4g_{X1}^3x_H^3x_\Phi^2 - 52g_1Xg_X^3g_{X1}^3x_H^3x_\Phi^2 \\
& - 52g_1g_X^2g_{X1}^3x_H^3x_\Phi^2 - 52g_1Xg_Xg_{X1}^4x_H^3x_\Phi^2 - 104g_1g_{X1}^5x_H^3x_\Phi^2 - 52g_X^6x_H^4x_\Phi^2 - 52g_X^4g_{X1}^2x_H^4x_\Phi^2 \\
& - 52g_X^2g_{X1}^4x_H^4x_\Phi^2 - 52g_{X1}^6x_H^4x_\Phi^2 - \frac{19}{4}g_1^4y_t^2 + \frac{21}{2}g_1^2g_2^2y_t^2 - \frac{9}{4}g_2^4y_t^2 - \frac{19}{2}g_1^2g_{1X}^2y_t^2 \\
& + \frac{21}{2}g_2^2g_{1X}^2y_t^2 - \frac{19}{4}g_{1X}^4y_t^2 - 38g_1^2g_1Xg_Xx_Hy_t^2 + 42g_2^2g_1Xg_Xx_Hy_t^2 - 38g_1^3g_X^3x_Hy_t^2 \\
& - 38g_1^3g_{X1}x_Hy_t^2 + 42g_1g_2^2g_{X1}x_Hy_t^2 - 38g_1g_1^2g_{X1}x_Hy_t^2 - 38g_1^2g_X^2x_H^2y_t^2 + 42g_2^2g_X^2x_H^2y_t^2 \\
& - 114g_1^2g_{1X}^2g_X^2x_H^2y_t^2 - 152g_1g_1Xg_Xg_{X1}^2x_H^2y_t^2 - 114g_1^2g_{X1}^2x_H^2y_t^2 + 42g_2^2g_{X1}^2x_H^2y_t^2 \\
& - 38g_1^2g_{1X}^2g_{X1}^2x_H^2y_t^2 - 152g_1Xg_X^3x_H^3y_t^2 - 152g_1g_X^2g_{X1}^3x_H^3y_t^2 - 152g_1Xg_Xg_{X1}^3x_H^3y_t^2 \\
& - 152g_1g_{X1}^3x_H^3y_t^2 - 76g_X^4x_H^4y_t^2 - 152g_X^2g_{X1}^4x_H^4y_t^2 - 76g_{X1}^4x_H^4y_t^2 - 5g_1^2g_1Xg_Xx_\Phi y_t^2 \\
& + 3g_2^2g_1Xg_Xx_\Phi y_t^2 - 5g_1^3g_Xx_\Phi y_t^2 - 5g_1^3g_{X1}x_\Phi y_t^2 + 3g_1g_2^2g_{X1}x_\Phi y_t^2 - 5g_1g_1^2g_{X1}x_\Phi y_t^2 \\
& - 10g_1^2g_X^2x_Hx_\Phi y_t^2 + 6g_2^2g_X^2x_Hx_\Phi y_t^2 - 30g_1^2g_X^2x_Hx_\Phi y_t^2 - 40g_1g_1Xg_Xg_{X1}x_Hx_\Phi y_t^2 \\
& - 30g_1^2g_{X1}^2x_Hx_\Phi y_t^2 + 6g_2^2g_{X1}^2x_Hx_\Phi y_t^2 - 10g_1^2g_{X1}^2x_Hx_\Phi y_t^2 - 60g_1Xg_X^3x_H^3x_\Phi y_t^2 \\
& - 60g_1g_X^2g_{X1}^2x_H^2x_\Phi y_t^2 - 60g_1Xg_Xg_{X1}^2x_H^2x_\Phi y_t^2 - 60g_1g_{X1}^3x_H^2x_\Phi y_t^2 - 40g_X^4x_H^3x_\Phi y_t^2 \\
& - 80g_X^2g_{X1}^3x_H^3x_\Phi y_t^2 - 40g_{X1}^4x_H^3x_\Phi y_t^2 - g_1^2g_X^2x_\Phi^2y_t^2 - 2g_1g_1Xg_Xg_{X1}^2x_\Phi^2y_t^2 - g_1^2g_{X1}^2x_\Phi^2y_t^2 \\
& - 4g_1Xg_X^3x_Hx_\Phi^2y_t^2 - 4g_1g_X^2g_{X1}^2x_Hx_\Phi^2y_t^2 - 4g_1Xg_Xg_{X1}^2x_Hx_\Phi^2y_t^2 - 4g_1g_{X1}^3x_Hx_\Phi^2y_t^2 \\
& - 4g_X^4x_H^2x_\Phi^2y_t^2 - 8g_X^2g_{X1}^2x_H^2x_\Phi^2y_t^2 - 4g_{X1}^4x_H^2x_\Phi^2y_t^2 - \frac{8}{3}g_1^2y_t^4 - 32g_3^2y_t^4 - \frac{8}{3}g_{1X}^2y_t^4 \\
& - \frac{32}{3}g_1Xg_Xx_Hy_t^4 - \frac{32}{3}g_1g_{X1}x_Hy_t^4 - \frac{32}{3}g_X^2x_H^2y_t^4 - \frac{32}{3}g_{X1}^2x_H^2y_t^4 - \frac{10}{3}g_1Xg_Xx_\Phi y_t^4 \\
& - \frac{10}{3}g_1g_{X1}x_\Phi y_t^4 - \frac{20}{3}g_X^2x_Hx_\Phi y_t^4 - \frac{20}{3}g_{X1}^2x_Hx_\Phi y_t^4 - \frac{2}{3}g_X^2x_\Phi^2y_t^4 - \frac{2}{3}g_{X1}^2x_\Phi^2y_t^4 + 30y_t^6 \\
& + \frac{629}{24}g_1^4\lambda_H + \frac{39}{4}g_1^2g_2^2\lambda_H - \frac{73}{8}g_2^4\lambda_H + \frac{69}{4}g_1^2g_{1X}^2\lambda_H + \frac{39}{4}g_2^2g_{1X}^2\lambda_H + \frac{629}{24}g_{1X}^4\lambda_H \\
& + 69g_1^2g_1Xg_Xx_H\lambda_H + 39g_2^2g_1Xg_Xx_H\lambda_H + \frac{629}{3}g_{1X}^3g_Xx_H\lambda_H + \frac{629}{3}g_1^3g_{X1}x_H\lambda_H \\
& + 39g_1g_2^2g_{X1}x_H\lambda_H + 69g_1g_{1X}^2g_{X1}x_H\lambda_H + 69g_1^2g_X^2x_H^2\lambda_H + 39g_2^2g_X^2x_H^2\lambda_H + 629g_{1X}^2g_X^2x_H^2\lambda_H
\end{aligned}$$

$$\begin{aligned}
& + 276g_1g_{1X}g_Xg_{X1}x_H^2\lambda_H + 629g_1^2g_{X1}^2x_H^2\lambda_H + 39g_2^2g_{X1}^2x_H^2\lambda_H + 69g_{1X}^2g_{X1}^2x_H^2\lambda_H \\
& + \frac{2516}{3}g_{1X}g_X^3x_H^3\lambda_H + 276g_1g_X^2g_{X1}x_H^3\lambda_H + 276g_{1X}g_Xg_{X1}^2x_H^3\lambda_H + \frac{2516}{3}g_1g_{X1}^3x_H^3\lambda_H \\
& + \frac{1258}{3}g_X^4x_H^4\lambda_H + 276g_X^2g_{X1}^2x_H^4\lambda_H + \frac{1258}{3}g_{X1}^4x_H^4\lambda_H + \frac{40}{3}g_{1X}^3g_Xx_\Phi\lambda_H + \frac{40}{3}g_1^3g_{X1}x_\Phi\lambda_H \\
& + 80g_{1X}^2g_X^2x_Hx_\Phi\lambda_H + 80g_1^2g_{X1}^2x_Hx_\Phi\lambda_H + 160g_{1X}g_X^3x_H^2x_\Phi\lambda_H + 160g_1g_{X1}^3x_H^2x_\Phi\lambda_H \\
& + \frac{320}{3}g_X^4x_H^3x_\Phi\lambda_H + \frac{320}{3}g_{X1}^4x_H^3x_\Phi\lambda_H + \frac{17}{2}g_{1X}^2g_X^2x_\Phi^2\lambda_H + \frac{17}{2}g_1^2g_{X1}^2x_\Phi^2\lambda_H + 34g_{1X}g_X^3x_Hx_\Phi^2\lambda_H \\
& + 34g_1g_{X1}^3x_Hx_\Phi^2\lambda_H + 34g_X^4x_H^2x_\Phi^2\lambda_H + 34g_{X1}^4x_H^2x_\Phi^2\lambda_H + \frac{85}{6}g_1^2y_t^2\lambda_H + \frac{45}{2}g_2^2y_t^2\lambda_H \\
& + 80g_3^2y_t^2\lambda_H + \frac{85}{6}g_{1X}^2y_t^2\lambda_H + \frac{170}{3}g_{1X}g_Xx_Hy_t^2\lambda_H + \frac{170}{3}g_1g_{X1}x_Hy_t^2\lambda_H + \frac{170}{3}g_X^2x_H^2y_t^2\lambda_H \\
& + \frac{170}{3}g_{X1}^2x_H^2y_t^2\lambda_H + \frac{25}{3}g_{1X}g_Xx_\Phi y_t^2\lambda_H + \frac{25}{3}g_1g_{X1}x_\Phi y_t^2\lambda_H + \frac{50}{3}g_X^2x_Hx_\Phi y_t^2\lambda_H \\
& + \frac{50}{3}g_{X1}^2x_Hx_\Phi y_t^2\lambda_H + \frac{5}{3}g_X^2x_\Phi^2y_t^2\lambda_H + \frac{5}{3}g_{X1}^2x_\Phi^2y_t^2\lambda_H - 3y_t^4\lambda_H + 36g_1^2\lambda_H^2 + 108g_2^2\lambda_H^2 \\
& + 36g_{1X}^2\lambda_H^2 + 144g_{1X}g_Xx_H\lambda_H^2 + 144g_1g_{X1}x_H\lambda_H^2 + 144g_X^2x_H^2\lambda_H^2 + 144g_{X1}^2x_H^2\lambda_H^2 - 144y_t^2\lambda_H^2 \\
& - 312\lambda_H^3 + 5g_{1X}^2g_X^2x_\Phi^2\lambda_{\text{mix}} + 10g_1g_{1X}g_Xg_{X1}x_\Phi^2\lambda_{\text{mix}} + 5g_1^2g_{X1}^2x_\Phi^2\lambda_{\text{mix}} + 20g_{1X}g_X^3x_Hx_\Phi^2\lambda_{\text{mix}} \\
& + 20g_1g_X^2g_{X1}x_Hx_\Phi^2\lambda_{\text{mix}} + 20g_{1X}g_Xg_{X1}^2x_Hx_\Phi^2\lambda_{\text{mix}} + 20g_1g_{X1}^3x_Hx_\Phi^2\lambda_{\text{mix}} + 20g_X^4x_H^2x_\Phi^2\lambda_{\text{mix}} \\
& + 40g_X^2g_{X1}^2x_H^2x_\Phi^2\lambda_{\text{mix}} + 20g_{X1}^4x_H^2x_\Phi^2\lambda_{\text{mix}} + 8g_X^2x_\Phi^2\lambda_{\text{mix}}^2 + 8g_{X1}^2x_\Phi^2\lambda_{\text{mix}}^2 - 12y_M^2\lambda_{\text{mix}}^2 \\
& - 10\lambda_H\lambda_{\text{mix}}^2 - 4\lambda_{\text{mix}}^3 \Big],
\end{aligned}$$

$$\begin{aligned}
\beta_{\lambda_\Phi}^{(2)} &= \frac{1}{(16\pi^2)^2} \cdot \frac{1}{3} \Big[ -334g_{1X}^2g_X^4x_\Phi^4 - 334g_1^2g_X^2g_{X1}^2x_\Phi^4 - 334g_{1X}^2g_X^2g_{X1}^2x_\Phi^4 - 334g_1^2g_{X1}^4x_\Phi^4 \\
& - 1336g_{1X}g_X^5x_Hx_\Phi^4 - 1336g_{1X}g_X^3g_{X1}^2x_Hx_\Phi^4 - 1336g_1g_X^2g_{X1}^3x_Hx_\Phi^4 - 1336g_1g_{X1}^5x_Hx_\Phi^4 \\
& - 1336g_X^6x_H^2x_\Phi^4 - 1336g_X^4g_{X1}^2x_H^2x_\Phi^4 - 1336g_X^2g_{X1}^4x_H^2x_\Phi^4 - 1336g_{X1}^6x_H^2x_\Phi^4 - 256g_{1X}g_X^5x_\Phi^5 \\
& - 256g_{1X}g_X^3g_{X1}^2x_\Phi^5 - 256g_1g_X^2g_{X1}^3x_\Phi^5 - 256g_1g_{X1}^5x_\Phi^5 - 512g_X^6x_Hx_\Phi^5 - 512g_X^4g_{X1}^2x_Hx_\Phi^5 \\
& - 512g_X^2g_{X1}^4x_Hx_\Phi^5 - 512g_{X1}^6x_Hx_\Phi^5 - 336g_X^6x_\Phi^6 - 696g_X^4g_{X1}^2x_\Phi^6 - 696g_X^2g_{X1}^4x_\Phi^6 - 336g_{X1}^6x_\Phi^6 \\
& + 144g_X^4x_\Phi^4y_M^2 + 288g_X^2g_{X1}^2x_\Phi^4y_M^2 + 144g_{X1}^4x_\Phi^4y_M^2 + 144g_X^2x_\Phi^2y_M^4 + 144g_{X1}^2x_\Phi^2y_M^4 + 2304y_M^6 \\
& + 30g_{1X}^2g_X^2x_\Phi^2\lambda_{\text{mix}} + 60g_1g_{1X}g_Xg_{X1}x_\Phi^2\lambda_{\text{mix}} + 30g_1^2g_{X1}^2x_\Phi^2\lambda_{\text{mix}} + 120g_{1X}g_X^3x_Hx_\Phi^2\lambda_{\text{mix}} \\
& + 120g_1g_X^2g_{X1}x_Hx_\Phi^2\lambda_{\text{mix}} + 120g_{1X}g_Xg_{X1}^2x_Hx_\Phi^2\lambda_{\text{mix}} + 120g_1g_{X1}^3x_Hx_\Phi^2\lambda_{\text{mix}} + 120g_X^4x_H^2x_\Phi^2\lambda_{\text{mix}} \\
& + 240g_X^2g_{X1}^2x_H^2x_\Phi^2\lambda_{\text{mix}} + 120g_{X1}^4x_H^2x_\Phi^2\lambda_{\text{mix}} + 12g_1^2\lambda_{\text{mix}}^2 + 36g_2^2\lambda_{\text{mix}}^2 + 12g_{1X}^2\lambda_{\text{mix}}^2 \\
& + 48g_{1X}g_Xx_H\lambda_{\text{mix}}^2 + 48g_1g_{X1}x_H\lambda_{\text{mix}}^2 + 48g_X^2x_H^2\lambda_{\text{mix}}^2 + 48g_{X1}^2x_H^2\lambda_{\text{mix}}^2 - 36y_t^2\lambda_{\text{mix}}^2 - 24\lambda_{\text{mix}}^3 \\
& + 211g_{1X}^2g_X^2x_\Phi^2\lambda_\Phi + 211g_1^2g_{X1}^2x_\Phi^2\lambda_\Phi + 844g_{1X}g_X^3x_Hx_\Phi^2\lambda_\Phi + 844g_1g_{X1}^3x_Hx_\Phi^2\lambda_\Phi \\
& + 844g_X^4x_H^2x_\Phi^2\lambda_\Phi + 844g_{X1}^4x_H^2x_\Phi^2\lambda_\Phi + 160g_{1X}g_X^3x_\Phi^3\lambda_\Phi + 160g_1g_{X1}^3x_\Phi^3\lambda_\Phi + 320g_X^4x_Hx_\Phi^3\lambda_\Phi \\
& + 320g_{X1}^4x_Hx_\Phi^3\lambda_\Phi + 396g_X^4x_\Phi^4\lambda_\Phi + 588g_X^2g_{X1}^2x_\Phi^4\lambda_\Phi + 396g_{X1}^4x_\Phi^4\lambda_\Phi + 90g_X^2x_\Phi^2y_M^2\lambda_\Phi \\
& + 90g_{X1}^2x_\Phi^2y_M^2\lambda_\Phi + 144y_M^4\lambda_\Phi - 60\lambda_{\text{mix}}^2\lambda_\Phi + 336g_X^2x_\Phi^2\lambda_\Phi^2 + 336g_{X1}^2x_\Phi^2\lambda_\Phi^2 \\
& - 720y_M^2\lambda_\Phi^2 - 720\lambda_\Phi^3 \Big],
\end{aligned}$$



$$\begin{aligned}
\beta_{\lambda_{\text{mix}}}^{(2)} = & \frac{1}{(16\pi^2)^2} \left[ -\frac{15}{4}g_1^2g_{1X}^2g_X^2x_\Phi^2 - \frac{45}{4}g_2^2g_{1X}^2g_X^2x_\Phi^2 - \frac{713}{12}g_{1X}^4g_X^2x_\Phi^2 - \frac{379}{6}g_1^3g_{1X}g_Xg_{X1}x_\Phi^2 \right. \\
& - \frac{45}{2}g_1g_2^2g_{1X}g_Xg_{X1}x_\Phi^2 - \frac{379}{6}g_1g_{1X}^3g_Xg_{X1}x_\Phi^2 - \frac{713}{12}g_1^4g_{X1}^2x_\Phi^2 - \frac{45}{4}g_1^2g_2^2g_{X1}^2x_\Phi^2 \\
& - \frac{15}{4}g_1^2g_{1X}^2g_{X1}^2x_\Phi^2 - 15g_1^2g_{1X}g_X^3x_Hx_\Phi^2 - 45g_2^2g_{1X}g_X^3x_Hx_\Phi^2 - \frac{1426}{3}g_{1X}^3g_X^3x_Hx_\Phi^2 \\
& - \frac{379}{3}g_1^3g_X^2g_{X1}x_Hx_\Phi^2 - 45g_1g_2^2g_X^2g_{X1}x_Hx_\Phi^2 - 394g_{1X}^2g_X^2g_{X1}x_Hx_\Phi^2 - 394g_1^2g_{1X}g_Xg_{X1}^2x_Hx_\Phi^2 \\
& - 45g_2^2g_{1X}g_Xg_{X1}^2x_Hx_\Phi^2 - \frac{379}{3}g_{1X}^3g_Xg_{X1}^2x_Hx_\Phi^2 - \frac{1426}{3}g_{1X}^3g_{X1}^3x_Hx_\Phi^2 - 45g_1g_2^2g_{X1}^3x_Hx_\Phi^2 \\
& - 15g_1g_{1X}^2g_{X1}^3x_Hx_\Phi^2 - 15g_1^2g_X^4x_H^2x_\Phi^2 - 45g_2^2g_X^4x_H^2x_\Phi^2 - 1426g_{1X}^2g_X^4x_H^2x_\Phi^2 \\
& - 818g_1g_{1X}g_X^3g_{X1}^2x_H^2x_\Phi^2 - 773g_1^2g_X^2g_{X1}^2x_H^2x_\Phi^2 - 90g_2^2g_X^2g_{X1}^2x_H^2x_\Phi^2 - 773g_{1X}^2g_X^2g_{X1}^2x_H^2x_\Phi^2 \\
& - 818g_1g_{1X}g_Xg_{X1}^3x_H^2x_\Phi^2 - 1426g_1^2g_{X1}^4x_H^2x_\Phi^2 - 45g_2^2g_{X1}^4x_H^2x_\Phi^2 - 15g_{1X}^2g_{X1}^4x_H^2x_\Phi^2 \\
& - \frac{5704}{3}g_{1X}g_X^5x_H^3x_\Phi^2 - \frac{1696}{3}g_{1X}g_X^4g_{X1}^3x_H^3x_\Phi^2 - 1576g_{1X}g_X^3g_{X1}^3x_H^3x_\Phi^2 - 1576g_{1X}g_X^2g_{X1}^3x_H^3x_\Phi^2 \\
& - \frac{1696}{3}g_{1X}g_Xg_{X1}^4x_H^3x_\Phi^2 - \frac{5704}{3}g_{1X}g_{X1}^5x_H^3x_\Phi^2 - \frac{2852}{3}g_X^6x_H^4x_\Phi^2 - \frac{3212}{3}g_X^4g_{X1}^2x_H^4x_\Phi^2 \\
& - \frac{3212}{3}g_X^2g_{X1}^4x_H^4x_\Phi^2 - \frac{2852}{3}g_{X1}^6x_H^4x_\Phi^2 - \frac{128}{3}g_{1X}^3g_X^3x_\Phi^3 - \frac{128}{3}g_1g_{1X}^2g_X^2g_{X1}x_\Phi^3 \\
& - \frac{128}{3}g_1^2g_{1X}g_Xg_{X1}^3x_\Phi^3 - \frac{128}{3}g_1^3g_{X1}^3x_\Phi^3 - 256g_{1X}^2g_X^4x_Hx_\Phi^3 - \frac{512}{3}g_1g_{1X}g_X^3g_{X1}x_Hx_\Phi^3 \\
& - \frac{256}{3}g_1^2g_X^2g_{X1}^2x_Hx_\Phi^3 - \frac{256}{3}g_{1X}g_X^2g_{X1}^2x_Hx_\Phi^3 - \frac{512}{3}g_1g_{1X}g_Xg_{X1}^3x_Hx_\Phi^3 - 256g_1^2g_{X1}^4x_Hx_\Phi^3 \\
& - 512g_{1X}g_X^5x_H^2x_\Phi^3 - \frac{512}{3}g_1g_X^4g_{X1}^2x_H^2x_\Phi^3 - \frac{1024}{3}g_{1X}g_X^3g_{X1}^2x_H^2x_\Phi^3 - \frac{1024}{3}g_1g_X^2g_{X1}^3x_H^2x_\Phi^3 \\
& - \frac{512}{3}g_{1X}g_Xg_{X1}^4x_H^2x_\Phi^3 - 512g_1g_{X1}^5x_H^2x_\Phi^3 - \frac{1024}{3}g_X^6x_H^3x_\Phi^3 - \frac{1024}{3}g_X^4g_{X1}^2x_H^3x_\Phi^3 \\
& - \frac{1024}{3}g_X^2g_{X1}^4x_H^3x_\Phi^3 - \frac{1024}{3}g_{X1}^6x_H^3x_\Phi^3 - 41g_{1X}^2g_X^4x_\Phi^4 - 56g_1g_{1X}g_X^3g_{X1}x_\Phi^4 - 15g_1^2g_X^2g_{X1}^2x_\Phi^4 \\
& - 15g_{1X}^2g_X^2g_{X1}^2x_\Phi^4 - 56g_1g_{1X}g_Xg_{X1}^3x_\Phi^4 - 41g_1^2g_{X1}^4x_\Phi^4 - 164g_{1X}g_X^5x_Hx_\Phi^4 - 112g_1g_X^4g_{X1}x_Hx_\Phi^4 \\
& - 172g_{1X}g_X^3g_{X1}^2x_Hx_\Phi^4 - 172g_1g_X^2g_{X1}^2x_Hx_\Phi^4 - 112g_{1X}g_Xg_{X1}^4x_Hx_\Phi^4 - 164g_1g_{X1}^5x_Hx_\Phi^4 \\
& - 164g_X^6x_H^2x_\Phi^4 - 284g_X^4g_{X1}^2x_H^2x_\Phi^4 - 284g_X^2g_{X1}^4x_H^2x_\Phi^4 - 164g_{X1}^6x_H^2x_\Phi^4 + 12g_{1X}^2g_X^2x_\Phi^2y_M^2 \\
& + 24g_1g_{1X}g_Xg_{X1}x_\Phi^2y_M^2 + 12g_1^2g_{X1}^2x_\Phi^2y_M^2 + 48g_{1X}g_X^3x_Hx_\Phi^2y_M^2 + 48g_1g_X^2g_{X1}x_Hx_\Phi^2y_M^2 \\
& + 48g_{1X}g_Xg_{X1}^2x_Hx_\Phi^2y_M^2 + 48g_1g_{X1}^3x_Hx_\Phi^2y_M^2 + 48g_X^4x_H^2x_\Phi^2y_M^2 + 96g_X^2g_{X1}^2x_H^2x_\Phi^2y_M^2 \\
& + 48g_{X1}^4x_H^2x_\Phi^2y_M^2 - 19g_{1X}^2g_X^2x_\Phi^2y_t^2 - 38g_1g_{1X}g_Xg_{X1}x_\Phi^2y_t^2 - 19g_1^2g_{X1}^2x_\Phi^2y_t^2 \\
& - 76g_{1X}g_X^3x_Hx_\Phi^2y_t^2 - 76g_1g_X^2g_{X1}x_Hx_\Phi^2y_t^2 - 76g_{1X}g_Xg_{X1}^2x_Hx_\Phi^2y_t^2 - 76g_1g_{X1}^3x_Hx_\Phi^2y_t^2 \\
& - 76g_X^4x_H^2x_\Phi^2y_t^2 - 152g_X^2g_{X1}^2x_H^2x_\Phi^2y_t^2 - 76g_{X1}^4x_H^2x_\Phi^2y_t^2 - 20g_{1X}g_X^3x_\Phi^3y_t^2 - 20g_1g_X^2g_{X1}x_\Phi^3y_t^2 \\
& - 20g_{1X}g_Xg_{X1}^3x_\Phi^3y_t^2 - 20g_1g_{X1}^3x_\Phi^3y_t^2 - 40g_X^4x_Hx_\Phi^3y_t^2 - 80g_X^2g_{X1}^2x_Hx_\Phi^3y_t^2 - 40g_{X1}^4x_Hx_\Phi^3y_t^2 \\
& - 4g_X^4x_\Phi^4y_t^2 - 8g_X^2g_{X1}^2x_\Phi^4y_t^2 - 4g_{X1}^4x_\Phi^4y_t^2 + 30g_{1X}^2g_X^2x_\Phi^2\lambda_H + 60g_1g_{1X}g_Xg_{X1}x_\Phi^2\lambda_H \\
& + 30g_1^2g_{X1}^2x_\Phi^2\lambda_H + 120g_{1X}g_X^3x_Hx_\Phi^2\lambda_H + 120g_1g_X^2g_{X1}x_Hx_\Phi^2\lambda_H + 120g_{1X}g_Xg_{X1}^2x_Hx_\Phi^2\lambda_H \\
& + 120g_1g_{X1}^3x_Hx_\Phi^2\lambda_H + 120g_X^4x_H^2x_\Phi^2\lambda_H + 240g_X^2g_{X1}^2x_H^2x_\Phi^2\lambda_H + 120g_{X1}^4x_H^2x_\Phi^2\lambda_H + \frac{557}{48}g_1^4\lambda_{\text{mix}} \Big]
\end{aligned}$$

$$\begin{aligned}
& + \frac{15}{8}g_1^2g_2^2\lambda_{\text{mix}} - \frac{145}{16}g_2^4\lambda_{\text{mix}} + \frac{45}{8}g_1^2g_{1X}\lambda_{\text{mix}} + \frac{15}{8}g_2^2g_{1X}\lambda_{\text{mix}} + \frac{557}{48}g_{1X}^4\lambda_{\text{mix}} \\
& + \frac{45}{2}g_1^2g_{1X}g_Xx_H\lambda_{\text{mix}} + \frac{15}{2}g_2^2g_{1X}g_Xx_H\lambda_{\text{mix}} + \frac{557}{6}g_{1X}^3g_Xx_H\lambda_{\text{mix}} + \frac{557}{6}g_{1X}^3g_{X1}x_H\lambda_{\text{mix}} \\
& + \frac{15}{2}g_1g_2^2g_{X1}x_H\lambda_{\text{mix}} + \frac{45}{2}g_1g_{1X}^2g_{X1}x_H\lambda_{\text{mix}} + \frac{45}{2}g_1^2g_X^2x_H^2\lambda_{\text{mix}} + \frac{15}{2}g_2^2g_X^2x_H^2\lambda_{\text{mix}} \\
& + \frac{557}{2}g_{1X}^2g_X^2x_H^2\lambda_{\text{mix}} + 90g_1g_{1X}g_Xg_{X1}x_H^2\lambda_{\text{mix}} + \frac{557}{2}g_1^2g_{X1}^2x_H^2\lambda_{\text{mix}} + \frac{15}{2}g_2^2g_{X1}^2x_H^2\lambda_{\text{mix}} \\
& + \frac{45}{2}g_{1X}^2g_{X1}^2x_H^2\lambda_{\text{mix}} + \frac{1114}{3}g_{1X}g_X^3x_H^3\lambda_{\text{mix}} + 90g_1g_X^2g_{X1}x_H^3\lambda_{\text{mix}} + 90g_{1X}g_Xg_{X1}^2x_H^3\lambda_{\text{mix}} \\
& + \frac{1114}{3}g_1g_{X1}^3x_H^3\lambda_{\text{mix}} + \frac{557}{3}g_X^4x_H^4\lambda_{\text{mix}} + 90g_X^2g_{X1}^2x_H^4\lambda_{\text{mix}} + \frac{557}{3}g_{X1}^4x_H^4\lambda_{\text{mix}} + \frac{20}{3}g_{1X}^3g_Xx_\Phi\lambda_{\text{mix}} \\
& + \frac{20}{3}g_1^3g_{X1}x_\Phi\lambda_{\text{mix}} + 40g_{1X}^2g_X^2x_Hx_\Phi\lambda_{\text{mix}} + 40g_1^2g_{X1}^2x_Hx_\Phi\lambda_{\text{mix}} + 80g_{1X}g_X^3x_H^2x_\Phi\lambda_{\text{mix}} \\
& + 80g_1g_{X1}^3x_H^2x_\Phi\lambda_{\text{mix}} + \frac{160}{3}g_X^4x_H^3x_\Phi\lambda_{\text{mix}} + \frac{160}{3}g_{X1}^4x_H^3x_\Phi\lambda_{\text{mix}} + \frac{497}{12}g_{1X}^2g_X^2x_\Phi^2\lambda_{\text{mix}} \\
& + 4g_1g_{1X}g_Xg_{X1}x_\Phi^2\lambda_{\text{mix}} + \frac{497}{12}g_1^2g_{X1}^2x_\Phi^2\lambda_{\text{mix}} + \frac{497}{3}g_{1X}g_X^3x_Hx_\Phi^2\lambda_{\text{mix}} + 8g_1g_X^2g_{X1}x_Hx_\Phi^2\lambda_{\text{mix}} \\
& + 8g_{1X}g_Xg_{X1}^2x_Hx_\Phi^2\lambda_{\text{mix}} + \frac{497}{3}g_1g_{X1}^3x_Hx_\Phi^2\lambda_{\text{mix}} + \frac{497}{3}g_X^4x_H^2x_\Phi^2\lambda_{\text{mix}} + 16g_X^2g_{X1}^2x_H^2x_\Phi^2\lambda_{\text{mix}} \\
& + \frac{497}{3}g_{X1}^4x_H^2x_\Phi^2\lambda_{\text{mix}} + \frac{80}{3}g_{1X}g_X^3x_\Phi^3\lambda_{\text{mix}} + \frac{80}{3}g_1g_{X1}^3x_\Phi^3\lambda_{\text{mix}} + \frac{160}{3}g_X^4x_Hx_\Phi^3\lambda_{\text{mix}} \\
& + \frac{160}{3}g_{X1}^4x_Hx_\Phi^3\lambda_{\text{mix}} + 42g_X^4x_\Phi^4\lambda_{\text{mix}} + 50g_X^2g_{X1}^2x_\Phi^4\lambda_{\text{mix}} + 42g_{X1}^4x_\Phi^4\lambda_{\text{mix}} + 15g_X^2x_\Phi^2y_M^2\lambda_{\text{mix}} \\
& + 15g_{X1}^2x_\Phi^2y_M^2\lambda_{\text{mix}} - 72y_M^4\lambda_{\text{mix}} + \frac{85}{12}g_1^2y_t^2\lambda_{\text{mix}} + \frac{45}{4}g_2^2y_t^2\lambda_{\text{mix}} + 40g_3^2y_t^2\lambda_{\text{mix}} \\
& + \frac{85}{12}g_{1X}^2y_t^2\lambda_{\text{mix}} + \frac{85}{3}g_{1X}g_Xx_Hy_t^2\lambda_{\text{mix}} + \frac{85}{3}g_1g_{X1}x_Hy_t^2\lambda_{\text{mix}} + \frac{85}{3}g_X^2x_H^2y_t^2\lambda_{\text{mix}} \\
& + \frac{85}{3}g_{X1}^2x_H^2y_t^2\lambda_{\text{mix}} + \frac{25}{6}g_{1X}g_Xx_\Phi y_t^2\lambda_{\text{mix}} + \frac{25}{6}g_1g_{X1}x_\Phi y_t^2\lambda_{\text{mix}} + \frac{25}{3}g_X^2x_Hx_\Phi y_t^2\lambda_{\text{mix}} \\
& + \frac{25}{3}g_{X1}^2x_Hx_\Phi y_t^2\lambda_{\text{mix}} + \frac{5}{6}g_X^2x_\Phi^2y_t^2\lambda_{\text{mix}} + \frac{5}{6}g_{X1}^2x_\Phi^2y_t^2\lambda_{\text{mix}} - \frac{27}{2}y_t^4\lambda_{\text{mix}} + 24g_1^2\lambda_H\lambda_{\text{mix}} \\
& + 72g_2^2\lambda_H\lambda_{\text{mix}} + 24g_{1X}^2\lambda_H\lambda_{\text{mix}} + 96g_{1X}g_Xx_H\lambda_H\lambda_{\text{mix}} + 96g_1g_{X1}x_H\lambda_H\lambda_{\text{mix}} + 96g_X^2x_H^2\lambda_H\lambda_{\text{mix}} \\
& + 96g_{X1}^2x_H^2\lambda_H\lambda_{\text{mix}} - 72y_t^2\lambda_H\lambda_{\text{mix}} - 60\lambda_H^2\lambda_{\text{mix}} + g_1^2\lambda_{\text{mix}}^2 + 3g_2^2\lambda_{\text{mix}}^2 + g_{1X}^2\lambda_{\text{mix}}^2 + 4g_{1X}g_Xx_H\lambda_{\text{mix}}^2 \\
& + 4g_1g_{X1}x_H\lambda_{\text{mix}}^2 + 4g_X^2x_H^2\lambda_{\text{mix}}^2 + 4g_{X1}^2x_H^2\lambda_{\text{mix}}^2 + 4g_X^2x_\Phi^2\lambda_{\text{mix}}^2 + 4g_{X1}^2x_\Phi^2\lambda_{\text{mix}}^2 - 24y_M^2\lambda_{\text{mix}}^2 \\
& - 12y_t^2\lambda_{\text{mix}}^2 - 72\lambda_H\lambda_{\text{mix}}^2 - 11\lambda_{\text{mix}}^3 + 20g_{1X}^2g_X^2x_\Phi^2\lambda_\Phi + 40g_1g_{1X}g_Xg_{X1}x_\Phi^2\lambda_\Phi + 20g_1^2g_{X1}^2x_\Phi^2\lambda_\Phi \\
& + 80g_{1X}g_X^3x_Hx_\Phi^2\lambda_\Phi + 80g_1g_X^2g_{X1}x_Hx_\Phi^2\lambda_\Phi + 80g_{1X}g_Xg_{X1}^2x_Hx_\Phi^2\lambda_\Phi + 80g_1g_{X1}^3x_Hx_\Phi^2\lambda_\Phi \\
& + 80g_X^4x_H^2x_\Phi^2\lambda_\Phi + 160g_X^2g_{X1}^2x_H^2x_\Phi^2\lambda_\Phi + 80g_{X1}^4x_H^2x_\Phi^2\lambda_\Phi + 64g_X^2x_\Phi^2\lambda_{\text{mix}}\lambda_\Phi + 64g_{X1}^2x_\Phi^2\lambda_{\text{mix}}\lambda_\Phi \\
& - 96y_M^2\lambda_{\text{mix}}\lambda_\Phi - 48\lambda_{\text{mix}}^2\lambda_\Phi - 40\lambda_{\text{mix}}\lambda_\Phi^2 \Big]. \tag{A.9}
\end{aligned}$$

## B THE SM RGEs AT TWO-LOOP LEVEL

The RGEs for coupling constants of the SM up to two-loop level [11] are give by

$$\begin{aligned}
\mu \frac{dg_3}{d\mu} &= \frac{g_3^3}{(4\pi)^2} \left[ -7 \right] + \frac{g_3^3}{(4\pi)^4} \left[ -26g_3^2 + \frac{9}{2}g_2^2 + \frac{11}{6}g_1^2 - 2y_t^2 \right], \\
\mu \frac{dg_2}{d\mu} &= \frac{g_2^3}{(4\pi)^2} \left[ -\frac{19}{6} \right] + \frac{g_2^3}{(4\pi)^4} \left[ 12g_3^2 + \frac{35}{6}g_2^2 + \frac{3}{2}g_1^2 - \frac{3}{2}y_t^2 \right], \\
\mu \frac{dg_1}{d\mu} &= \frac{g_1^3}{(4\pi)^2} \left[ \frac{41}{6} \right] + \frac{g_1^3}{(4\pi)^4} \left[ \frac{44}{3}g_3^2 + \frac{9}{2}g_2^2 + \frac{199}{18}g_1^2 - \frac{17}{6}y_t^2 \right], \\
\mu \frac{dy_t}{d\mu} &= \frac{y_t}{(4\pi)^2} \left[ \frac{9}{2}y_t^2 - 8g_3^2 - \frac{9}{4}g_2^2 - \frac{17}{12}g_1^2 \right] \\
&+ \frac{y_t}{(4\pi)^4} \left[ y_t^2 \left( -12y_t^2 - 12\lambda_H + 36g_3^2 + \frac{225}{16}g_2^2 + \frac{131}{16}g_1^2 \right) \right. \\
&+ \left. 6\lambda_H^2 - 108g_3^4 - \frac{23}{4}g_2^4 + \frac{1187}{216}g_1^4 + 9g_3^2g_2^2 + \frac{19}{9}g_3^2g_1^2 - \frac{3}{4}g_2^2g_1^2 \right], \\
\mu \frac{d\lambda_H}{d\mu} &= \frac{1}{(4\pi)^2} \left[ \lambda_H \left( 24\lambda_H + 12y_t^2 - 9g_2^2 - 3g_1^2 \right) - 6y_t^4 + \frac{9}{8}g_2^4 + \frac{3}{8}g_1^4 + \frac{3}{4}g_2^2g_1^2 \right] \\
&+ \frac{1}{(4\pi)^4} \left[ \lambda_H^2 \left( -312\lambda_H - 144y_t^2 + 108g_2^2 + 36g_1^2 \right) \right. \\
&+ \lambda_H y_t^2 \left( -3y_t^2 + 80g_3^2 + \frac{45}{2}g_2^2 + \frac{85}{6}g_1^2 \right) + \lambda_H \left( -\frac{73}{8}g_2^4 + \frac{629}{24}g_1^4 + \frac{39}{4}g_1^2g_2^2 \right) \\
&+ y_t^4 \left( 30y_t^2 - 32g_3^2 - \frac{8}{3}g_1^2 \right) + y_t^2 \left( -\frac{9}{4}g_2^4 - \frac{19}{4}g_1^4 + \frac{21}{2}g_2^2g_1^2 \right) \\
&+ \left. \frac{305}{16}g_2^6 - \frac{379}{48}g_1^6 - \frac{289}{48}g_2^4g_1^2 - \frac{559}{48}g_2^2g_1^4 \right]. \tag{B.1}
\end{aligned}$$

In our analysis, we numerically solve these SM RGEs with the following boundary conditions at  $\mu = m_t$  [11]<sup>5</sup>

$$\begin{aligned}
g_3(m_t) &= 1.1666 + 0.00314 \left( \frac{\alpha_3(m_Z) - 0.1184}{0.0007} \right) - 0.00046 \left( \frac{m_t}{\text{GeV}} - 173.34 \right), \\
g_2(m_t) &= 0.64779 + 0.00004 \left( \frac{m_t}{\text{GeV}} - 173.34 \right) + 0.00011 \left( \frac{m_W - 80.384\text{GeV}}{0.014\text{GeV}} \right), \\
g_1(m_t) &= 0.35830 + 0.00011 \left( \frac{m_t}{\text{GeV}} - 173.34 \right) - 0.00020 \left( \frac{m_W - 80.384\text{GeV}}{0.014\text{GeV}} \right), \\
y_t(m_t) &= 0.93690 + 0.00556 \left( \frac{m_t}{\text{GeV}} - 173.34 \right) - 0.00042 \left( \frac{\alpha_3(m_Z) - 0.1184}{0.0007} \right), \\
\lambda_H(m_t) &= 0.12604 + 0.00206 \left( \frac{m_h}{\text{GeV}} - 125.15 \right) - 0.00004 \left( \frac{m_t}{\text{GeV}} - 173.34 \right), \tag{B.2}
\end{aligned}$$

---

<sup>5</sup>We employed the boundary conditions in arXiv:1307.3536v4.

using the inputs,  $\alpha_3(m_Z) = 0.1184$ ,  $m_t = 173.34$  GeV,  $m_h = 125.09$  GeV, and  $m_W = 80.384$  GeV.

## References

- [1] W. A. Bardeen, “On naturalness in the standard model,” Report No. FERMILAB-CONF-95-391-T.
- [2] S. R. Coleman and E. J. Weinberg, “Radiative corrections as the origin of spontaneous symmetry breaking,” *Phys. Rev. D* **7**, 1888 (1973).
- [3] K. Fujikawa, “Heavy fermions in the standard sequential scheme,” *Prog. Theor. Phys.* **61**, 1186 (1979).
- [4] R. Hempfling, “The next-to-minimal Coleman-Weinberg model,” *Phys. Lett. B* **379**, 153 (1996) [arXiv:hep-ph/9604278]; J. R. Espinosa and M. Quiros, “Novel effects in electroweak breaking from a hidden sector,” *Phys. Rev. D* **76**, 076004 (2007) [arXiv:hep-ph/0701145]; W. F. Chang, J. N. Ng, and J. M. S. Wu, “Shadow Higgs boson from a scale-invariant hidden U(1)s model,” *Phys. Rev. D* **75**, 115016 (2007) [arXiv:hep-ph/0701254]; R. Foot, A. Kobakhidze, and R. R. Volkas, “Electroweak Higgs as a pseudo-Goldstone boson of broken scale invariance,” *Phys. Lett. B* **655**, 156 (2007) [arXiv:0704.1165 [hep-ph]]; R. Foot, A. Kobakhidze, K. L. McDonald, and R. R. Volkas, “Neutrino mass in radiatively broken scale-invariant models,” *Phys. Rev. D* **76**, 075014 (2007) [arXiv:0706.1829 [hep-ph]]; “Solution to the hierarchy problem from an almost decoupled hidden sector within a classically scale invariant theory,” *Phys. Rev. D* **77**, 035006 (2008) [arXiv:0709.2750 [hep-ph]]; K. A. Meissner and H. Nicolai, “Conformal symmetry and the standard model,” *Phys. Lett. B* **648**, 312 (2007) [arXiv:hep-th/0612165]; “Effective action, conformal anomaly and the issue of quadratic divergences,” *Phys. Lett. B* **660**, 260 (2008) [arXiv:0710.2840 [hep-th]]; “Neutrinos, axions and conformal symmetry,” *Eur. Phys. J. C* **57**, 493 (2008) [arXiv:0803.2814 [hep-th]]; M. Holthausen, M. Lindner, and M. A. Schmidt, “Radiative symmetry breaking of the minimal left-right symmetric model,” *Phys. Rev. D* **82**, 055002 (2010) [arXiv:0911.0710 [hep-ph]]; M. Heikinheimo, A. Racioppi, C. Spethmann, M. Raidal, and K. Tuominen, “Physical naturalness and dynamical breaking of classical scale invariance,” *Mod. Phys. Lett. A* **29**, 1450077 (2014) [arXiv:1304.7006 [hep-ph]] ; A. Farzinnia, H. J. He, and J. Ren, “Natural electroweak symmetry breaking from scale invariant Higgs mechanism,” *Phys. Lett. B* **727**, 141 (2013) [arXiv:1308.0295 [hep-ph]]; E. Gabrielli, M. Heikinheimo, K. Kannike, A. Racioppi, M. Raidal, and C. Spethmann, “Towards completing the standard model: Vacuum stability, electroweak symmetry breaking, and dark matter,” *Phys. Rev. D* **89**, no. 1, 015017 (2014) [arXiv:1309.6632 [hep-ph]] ; A. Farzinnia and J. Ren, “Higgs partner searches and dark matter phenomenology in a classically scale invariant Higgs boson sector,” *Phys. Rev. D* **90**, no. 1, 015019 (2014) [arXiv:1405.0498 [hep-ph]]; M. Lindner, S. Schmidt, and J. Smirnov, “Neutrino masses and conformal electro-weak symmetry breaking,” *J. High Energy Phys.* **10** (2014) 177 [arXiv:1405.6204 [hep-ph]]; W. Altmannshofer, W. A. Bardeen, M. Bauer, M. Carena,

- and J. D. Lykken, “Light dark matter, naturalness, and the radiative origin of the electroweak scale,” J. High Energy Phys. 01 (2015) 032 [arXiv:1408.3429 [hep-ph]]; F. Goertz, “Electroweak symmetry breaking without the  $\mu^2$  term,” arXiv:1504.00355 [hep-ph]; N. Haba, H. Ishida, N. Okada and Y. Yamaguchi, “Bosonic seesaw mechanism in a classically conformal extension of the Standard Model,” Phys. Lett. B **754**, 349 (2016) doi:10.1016/j.physletb.2016.01.050 [arXiv:1508.06828 [hep-ph]]; “Electroweak symmetry breaking through bosonic seesaw mechanism in a classically conformal extension of the Standard Model,” arXiv:1509.01923 [hep-ph]; A. Das, N. Okada, and N. Papapietro, “Electroweak vacuum stability in classically conformal  $B - L$  extension of the standard model,” arXiv:1509.01466 [hep-ph]; H. Okada, Y. Orikasa and K. Yagyu, “Higgs Triplet Model with Classically Conformal Invariance,” arXiv:1510.00799 [hep-ph]; N. Haba, H. Ishida, R. Takahashi and Y. Yamaguchi, “Gauge coupling unification in a classically scale invariant model,” JHEP **1602**, 058 (2016) doi:10.1007/JHEP02(2016)058 [arXiv:1511.02107 [hep-ph]]; N. Haba, H. Ishida, N. Kitazawa and Y. Yamaguchi, “A new dynamics of electroweak symmetry breaking with classically scale invariance,” Phys. Lett. B **755**, 439 (2016) doi:10.1016/j.physletb.2016.02.052 [arXiv:1512.05061 [hep-ph]].
- [5] V. V. Khoze, C. McCabe, and G. Ro, “Higgs vacuum stability from the dark matter portal,” J. High Energy Phys. 08 (2014) 026 [arXiv:1403.4953 [hep-ph]].
- [6] S. Iso, N. Okada, and Y. Orikasa, “Classically conformal  $B - L$  extended standard model,” Phys. Lett. B **676**, 81 (2009) [arXiv:0902.4050 [hep-ph]]; “Minimal B-L model naturally realized at the TeV scale,” Phys. Rev. D **80**, 115007 (2009) [arXiv:0909.0128 [hep-ph]].
- [7] S. Oda, N. Okada and D. s. Takahashi, “Classically conformal  $U(1)'$  extended standard model and Higgs vacuum stability,” Phys. Rev. D **92**, no. 1, 015026 (2015), [arXiv:1504.06291 [hep-ph]].
- [8] T. Appelquist, B. A. Dobrescu, and A. R. Hopper, “Nonexotic neutral gauge bosons,” Phys. Rev. D **68**, 035012 (2003) [hep-ph/0212073].
- [9] P. Minkowski, “ $\mu \rightarrow e\gamma$  at a rate of one out of  $10^9$  muon decays?,” Phys. Lett. B **67**, 421 (1977); T. Yanagida, “Horizontal gauge symmetry and masses of neutrinos,” in *Proceedings of the Workshop on the Unified Theory and the Baryon Number in the Universe*, edited by O. Sawada and A. Sugamoto (KEK, Tsukuba, Japan, 1979), p. 95; M. Gell-Mann, P. Ramond, and R. Slansky, “Complex spinors and unified theories,” in *Supergravity*, edited by P. van Nieuwenhuizen *et al.* (North Holland, Amsterdam, 1979), p. 315; S. L. Glashow, “The future of elementary particle physics,” in *Proceedings of the 1979 Cargèse Summer Institute on Quarks and Leptons*, edited by M. Lévy *et al.* (Plenum Press, New York, 1980), p. 687; R. N. Mohapatra and G. Senjanović, “Neutrino mass and spontaneous parity nonconservation,” Phys. Rev. Lett. **44**, 912 (1980).
- [10] G. Aad *et al.* (ATLAS and CMS Collaborations), “Combined measurement of the Higgs boson mass in  $pp$  collisions at  $\sqrt{s} = 7$  and 8 TeV with the ATLAS and CMS experiments,” Phys. Rev. Lett. **114**, 191803 (2015) [arXiv:1503.07589 [hep-ex]].

- [11] D. Buttazzo, G. Degrandi, P. P. Giardino, G. F. Giudice, F. Sala, A. Salvio, and A. Strumia, “Investigating the near-criticality of the Higgs boson,” *J. High Energy Phys.* **12** (2013) 089 [We used the following updated version of the published paper: arXiv:1307.3536v4].
- [12] ATLAS and CDF and CMS and D0 Collaborations, “First combination of Tevatron and LHC measurements of the top-quark mass,” arXiv:1403.4427 [hep-ex].
- [13] J. Elias-Miro, J. R. Espinosa, G. F. Giudice, G. Isidori, A. Riotto, and A. Strumia, “Higgs mass implications on the stability of the electroweak vacuum,” *Phys. Lett. B* **709**, 222 (2012) [arXiv:1112.3022 [hep-ph]].
- [14] LEP and ALEPH and DELPHI and L3 and OPAL and LEP Electroweak Working Group and SLD Electroweak Group and Heavy Flavor Group Collaborations, “A combination of preliminary electroweak measurements and constraints on the standard model,” arXiv:hep-ex/0312023.
- [15] M. Carena, A. Daleo, B. A. Dobrescu, and T. M. P. Tait, “ $Z'$  gauge bosons at the Fermilab Tevatron,” *Phys. Rev. D* **70**, 093009 (2004) [arXiv:hep-ph/0408098].
- [16] ALEPH Collaboration, DELPHI Collaboration, L3 Collaboration, OPAL Collaboration, LEP Electroweak Working Group, “Electroweak measurements in electron-positron collisions at W-boson-pair energies at LEP,” *Phys. Rep.* **532** (2013) 119, [arXiv:hep-ex/1302.3415].
- [17] ATLAS collaboration, “Search for new phenomena in the dilepton final state using proton-proton collisions at  $\sqrt{s} = 13$  TeV with the ATLAS detector,” ATLAS-CONF-2015-070.
- [18] CMS Collaboration, “Search for a narrow resonance produced in 13 TeV pp collisions decaying to electron pair or muon pair final states,” CMS-PAS-EXO-15-005.
- [19] C. Coriano, L. D. Rose, and C. Marzo, “Vacuum stability in U(1)-prime extensions of the standard model with TeV scale right handed neutrinos,” *Phys. Lett. B* **738**, 13 (2014) [arXiv:1407.8539 [hep-ph]].
- [20] S. D. Chiara, V. Keus, and O. Lebedev, “Stabilizing the Higgs potential with a  $Z'$ ,” *Phys. Lett. B* **744**, 59 (2015) [arXiv:1412.7036 [hep-ph]].
- [21] F. Staub, “SARAH 3.2: Dirac gauginos, UFO output, and more,” *Comput. Phys. Commun.* **184**, pp. 1792 (2013), [arXiv:1207.0906 [hep-ph]]; “SARAH 4: A tool for (not only SUSY) model builders,” *Comput. Phys. Commun.* **185**, 1773 (2014), [arXiv:1309.7223 [hep-ph]].
- [22] CMS Collaboration, “Search for resonances in the dilepton mass distribution in pp collisions at  $\sqrt{s} = 8$  TeV,” Report No. CMS-PAS-EXO-12-061; V. Khachatryan *et al.* (CMS Collaboration), “Search for physics beyond the standard model in dilepton mass spectra in proton-proton collisions at  $\sqrt{s} = 8$  TeV,” *JHigh Energy Phys.* **04** (2015) 025 [arXiv:1412.6302 [hep-ex]].

- [23] G. Aad *et al.* (ATLAS Collaboration), “Search for high-mass dilepton resonances in pp collisions at  $\sqrt{s} = 8$  TeV with the ATLAS detector,” Phys. Rev. D **90**, no. 5, 052005 (2014) [arXiv:1405.4123 [hep-ex]].
- [24] V. D. Barger, W. Y. Keung and E. Ma, “Doubling of weak gauge bosons in an extension of the standard model,” Phys. Rev. Lett. **44**, 1169 (1980).
- [25] J. Pumplin, D. R. Stump, J. Huston, H. L. Lai, P. Nadolsky and W. K. Tung, “New generation of parton distributions with uncertainties from global QCD analysis,” JHEP **07** (2002) 012.
- [26] N. Okada and S. Okada, “ $Z'_{BL}$  portal dark matter and LHC Run-2 results,” Phys. Rev. D **93**, no. 7, 075003 (2016) doi:10.1103/PhysRevD.93.075003 [arXiv:1601.07526 [hep-ph]].
- [27] J. A. Casas, J. R. Espinosa, and I. Hidalgo, “Implications for new physics from fine-tuning arguments. I: Application to SUSY and seesaw cases,” J. High Energy Phys. 11 (2004) 057 [arXiv:hep-ph/0410298].